Earth's First Snowball Event: Evidence from the Early Paleoproterozoic Huronian Supergroup

Sophie Kurucz[1], Philip Fralick[1*], Martin Homann[2] and Stefan Lalonde[3]

[1]Department of Geology, Lakehead University, Thunder Bay, Ontario, Canada, skurucz@lakeheadu.ca, philip.fralick@lakeheadu.ca

[2]Earth Sciences, University College London, London, UK, m.homann@ucl.ac.uk

[3]European Institute for Marine Studies, CNRS-UMR6538, Laboratoire Géosciences Océan, Brest, France, stefan.lalonde@univ.brest.fr

* Corresponding Author

Abstract

Ever since it was first proposed that the Earth completely froze during glaciations ~640 million years ago evidence supporting this hypothesis has been increasing, primarily from samples of carbonates directly overlying glacial diamictites, termed cap carbonates. However, this was not the first extensive glacial period that affected planet Earth: ~1750 million years prior to Neoproterozoic glaciations the Earth went through its first major glacial episode, the early Paleoproterozoic Huronian glaciations. The second Huronian ice advance deposited the Bruce Formation, with its overlying cap carbonate, the Espanola Formation. This up to ~300 m thick succession of limestone, siltstone, dolostone and sandstone overlies diamictite containing a

dropstone-bearing layer with $\delta^{13}C_{carb}$ of -10‰. The ^{12}C-enriched interval also has rare earth element (REE) patterns with negative Eu anomalies, radiogenic Sr isotopes, and negative εNd(0) in the carbonate. The first of these observations is probably due to highly reducing conditions in the sediment, and the possible thawing of methane-rich areas, releasing fluids that mixed with the overlying bottom waters; the last two reflect the diagenetic incorporation into the carbonate of radiogenic Sr, and derivation of REEs, including Nd, from abundant silty loess. This infers a stratified water mass with a relatively stagnant bottom layer during disintegration of an ice shelf. Above this REE patterns through the basal Espanola become increasingly more light depleted upwards, C becomes heavier, Sr is less radiogenic, εNd(0) is near 0 and one area has up to ~1300ppm Ba incorporated into the carbonate, indicating breakdown of water-mass stratification. Vertically over ~200m $\delta^{13}C_{carb}$ increases from -4.5 to -2.5‰ as the environment shallowed incorporating gradually increasing amounts of seawater into the freshwater plume, which initially extended to depths below wave base. Strata deposited in the upper Espanola near the strandline contain layers of Fe-Mn-rich dolomite with positive Eu anomalies reflecting Paleoproterozioc seawater composition dominating even the nearshore by this time. These observations are similar to those from Neoproterozoic cap carbonates, and provide new evidence for the possibly snowball Earth-like nature of the ~2.4 Ga Bruce glaciation.

Keywords: Snowball Earth, Paleoproterozoic Glaciations, Huronian Supergroup, Espanola Formation, Precambrian Glaciology, Cap Carbonates

1.1 Introduction

Ever since Kirschvink (1992) and Hoffman et al. (1998) first proposed that the Earth completely froze during the Marinoan glaciation (635.5±0.6 and 636.3±4.9 million years ago, Hoffmann et al., 2004 ; Zhang et al., 2008; respectively) and the Sturtian glaciation (716±1 and 716.47±0.24, Denyszyn et al. 2009; Macdonald et al., 2010; respectively), evidence supporting this hypothesis has been increasing, primarily from samples of directly overlying carbonates, termed cap carbonates, collected at various locations throughout the planet. Carbon isotopes (Yoshioka et al., 2003), Sr and Nd isotopes (Yoshioka et al., 2003; Liu et al., 2014; Wen et al., 2015; Hu et al., 2016; Caxito et al., 2018; Liu et al., 2018; Wei et al., 2019), and REE patterns (Rodler et al., 2016; Hu et al., 2016; Caxito et al., 2018) all indicate that the cap carbonates overlying the Marinoan and Sturtian glacial events were deposited from water that had a significant freshwater influence. This influence was probably the result of melting of extensive glacial ice causing salinity stratification of the world ocean (Shields, 2005), with the non-saline waters extending down to sub-continental shelf depths (Liu et al., 2018, Fig. 7A). Though there is still controversy as to whether the Earth experienced a snowball (Hoffman et al, 1998; Hoffman and Schrag, 2002), or a slushball (Hyde et al., 2000; Arne and Montenari, 2008) with incomplete freezing (Eyles and Januszczak, 2004), the evidence strongly indicates extensive glacial ice developed and, upon melting, non-marine water from this event dominated shelf environments (Shields, 2005).

This was not the first extensive glacial period that effected planet Earth. Approximately 1.6 Ga prior to these Neoproterozoic glaciations the Earth went through its first major glacial episode, the early Paleoproterozoic Huronian glaciations (Roscoe, 1973). This series of at least four glacial advances (Ramsay Lake Formation, Bruce Formation and two advances in the Gowganda

Formation separated by extensive marine and deltaic deposits) was driven by the Great Oxidation Event (GOE), wherein significant amounts of free oxygen built up in the atmosphere (Farquhar et al., 2000). Prior to this, oxidation of the sink of reduced gases in the atmosphere was necessary, thus destroying methane and leading to the temperature crash (Kirschvink et al., 2000; Zahnle et al., 2006). Evidence for the first appearance of the GOE is present in the Huronian Supergroup, an up to 12 km thick succession of sedimentary and volcanic rocks (Figure 1) deposited on the margin of Superior craton (Figure 2) between 2.45 and 2.31 Ga (Krough et al., 1984; Rasmussen et al., 2013; respectively). The first evidence for the GOE in the Huronian Supergroup probably occurs following the second glacial episode (Papineau et al., 2007), though more recent investigations (Cui et al., 2017) indicate disappearance of the sulfur mass independent fractionation (MIF) signal, heralding ozone buildup in the atmosphere, may not arise till the next glacial interval. However, multiple sulfur isotopic data from Paleoproterozoic units in South Africa (Bekker et al., 2004) agree with Papineau et al.'s (2007) positioning of the MIF-MDF transition in the Huronian interglacial Espanola Formation above the glacial Bruce Formation (Figure 2). This is in contrast to multiple sulfur isotopic measurements conducted on Paleoproterozoic units in the Fennoscandian Shield that place the transition to the GOE prior to the Huronian glacial events (Warke et al., 2020).

The possibility that the Paleoproterozoic glacial episodes represent world-wide freezing of the planet has been previously put forward and debated (Kirschvink et al., 2000; Bekker et al., 2001, 2005; Kopp et al., 2005; Hoffman, 2013; Young, 2013b, 2014). No consensus has developed from these investigations and resulting conclusions, which in some instances are mutually exclusive. This highlights the need for more data on the Paleoproterozoic glacial cycles, and in particular the associated possible cap carbonates. Here we present a detailed study of the

Paleoproterozoic, Huronian, Espanola Formation, a thick carbonate succession overlying the Bruce Formation glaciogenic diamictites.

Previous evidence for the Huronian Supergroup glacial deposits representing a global freezing event was based largely on paleolatitude data that indicate deposition occurred within 11˚ of the paleoequator (Williams and Schmidt, 1997). However, the results of this study have come into contention due to a negative fold test (Hilburn et al., 2005), though paleolatitude data collected from the 2.45 Ga Matachewan dykes of Superior Province provided a latitude of ~5.5˚, reinforcing a position near the equator (Bates and Halls, 1990). In addition, correlative glacial units of the Kaapvaal Craton were deposited in a near equatorial position (Evans et al., 1997), and reconstruction of landmass positioning at this time places many of the cratons close to the equator (Gumsley et al., 2017).

Geochemical evidence from the Espanola cap carbonate, and its correlative units the Vagner and Bottle Creek Formations of the Snowy Pass Supergroup in the Medicine Bow Mountains and Sierra Madre, U.S.A., relevant to whether there was a Paleoproterozoic snowball event, is limited. Bekker (Bekker and Karhu, 1996; Bekker et al., 1999, 2001, 2005) provided $\delta^{13}C$ data for these formations and used their light carbon values to support the possibility of a snowball event. This was tempered by the apparent lack of an upward increase in the values, a typical pattern present in Neoproterozoic cap carbonates (cf. Kennedy, 1996; Hoffman et al., 1998; Halverson et al., 2002). Young (2013a), as an argument for deposition of the Espanola in a rift basin and it not being a cap carbonate similar to those in the Neoproterozoic, used the presence of light rare earth element depletion in an Espanola sample as evidence for a strong hydrothermal

influence on the depositing fluids. He also suggested that the enrichment of Fe and Mn and the presence of positive Eu anomalies in dolostone samples was evidence of hydrothermal activity during deposition of the Espanola Formation carbonates and this indicated deposition in a hydrothermally active rift, with Bruce glaciation occurring due to a cold climate on the thermally domed edge of the rift (Young, 2014). However, these geochemical features are common in sediments precipitated from the early Paleoproterozoic ocean (Planavsky et al., 2010) and both an enrichment of Fe and Mn and mild to strong positive Eu anomalies are present within some Neoproterozoic cap carbonates (cf. Huang et al., 2011; Meyer et al., 2012; Verdel et al., 2018).

The possibility that the Bruce-Espanola glacial cycle was deposited in an isolated rift basin is important to whether it represents a Paleoproterozoic snowball Earth event, as without connection to the world ocean any geochemical anomalies would only be of local significance. The core of this is a disagreement as to when the transition from rift to divergent margin developed. Most authors (Fralick and Miall, 1981; Fralick, 1984; Miall, 1985; Fralick and Miall, 1989; Bennett et al., 1991; Hoffman, 2013) place the rift to drift transition at the base of the Matinenda Formation. However, Young and others (Young and Nesbitt, 1985; Young et al., 2001; Young, 2004; Young, 2014) favour the transition to have occurred at the base of the Gowganda Formation (Figure 2). Hoffman (2013) discusses reasons why this is unlikely. In addition to his arguments, there is a change from very locally sourced detritus in the rift-fill Livingston Creek Formation (Bennett, 2006) to the overlying Matinenda Formation, which has much further traveled clasts of resistate lithogolies (Fralick and Miall, 1989) similar to compositionally mature sediments common in early drift-stage basins (Dickinson, 1985; Bond et al. 1995) and not rift basins. Oxygen isotopes in quartz sand and pebbles also denote a profound

change in source area from deposition of the Livingston Creek Formation to that of the Matinenda Formation (Vennemann et al., 1996). Rifts developed prior to continental separation commonly form on top of thermal welts (Closs, 1939; e.g. Wilson, 1975; Thiessen et al., 1979; Omar et al., 1989; Davis and Slack, 2002; Chorowicz, 2005; Pik et al., 2008), which limit stream entry to the basin (Angelier, 1985; Steckler, 1985; Cox, 1989; Kent, 1991; Axen et al., 2000) resulting in locally sourced detritus in the rift sediment (Sellwood and Netherwood, 1984; Ori, 1989; Favre and Stampfli, 1992; Steckler and Omar, 1994), similar to the Livingston Creek Formation. Further travelled detritus, e.g. that of the Matinenda Formation, commonly only enters after thermal decay, which occurs during drift (Steckler and Watts, 1978; Royden et al., 1980). Also, a comparison with the Mesozoic sediments forming the rift to divergent margin basins of Atlantic Canada and the United States highlights that the rift portion of the succession is commonly thin compared to the drift component (Hutchinson et al., 1980, see also Bond et al., 1995, Fig. 4.1). For example, the rift sediments and volcanics in the large Mesozoic to Cenozoic Scotia Basin on the northern Atlantic passive margin are 3 to 5 km thick, whereas the Jurassic portion of the post-rift successions is up to approximately 13 km, with many kilometers of Cretaceous and Cenozoic strata overlying that (Wade et al., 1995). This is because crustal flexure and stretching during the rift phase can only drive subsidence to a limited degree (Royden and Keen, 1980). However, the amount of subsidence caused by thermal decay and sediment loading during divergent movement is much more significant (Sleep 1971; Steckler and Watts, 1978). This has bearing on the time scale as well. The rift phase of the Scotia Basin, including volcanism, only lasted for 15 My, whereas the divergent margin phase received most of its sediment over the following approximately 100 My (Wade and MacLean, 1990; Wade et al., 1995; Labails et al., 2010; Campbell et al., 2015), with correlative basins in Morocco recording

similar time-frames (Medina, 1995). Huronian sedimentation and volcanism occurred over a minimum of 140 Ma, and by comparison with the Mesozoic eastern Canadian rift to divergent margin, the vast majority of that time and stratigraphic succession should be represented by the divergent margin sediments. In addition, the Jurassic volcanism on the U.S. Atlantic margin, Canadian margin and Moroccan margin overlaps the rift basins and is overlapped itself by the earliest drift-stage strata (Bond et al., 1995, p. 169; Campbell et al., 2015; Medina, 1995; respectively). In the Huronian, the Livingston Creek rift fanglomerates lie below the Thessalon Volcanics and the Matinenda Formation lies above them, by analogy placing the rift to drift transition at the base of the Matinenda. Thus, having the majority of sediments in the Huronian deposited during the rift phase is incongruent with the processes and products that operate and are present on more recent divergent systems, confirming the Bruce-Espanola glacial cycle would have operated on a divergent margin open to the world ocean (Fralick and Miall, 1981; Fralick, 1984; Miall, 1985; Fralick and Miall, 1989; Bennett et al., 1991; Hoffman, 2013).

The existence of numerous Paleoproterozoic glaciogenic units on diverse cratons that are chronostratigraphicly correlative and equatorial (see Gumsley et al., 2017,for a review) is difficult to explain without widespread, not localized, glaciations. These deposits have been found in Canada (Miall, 1983), the United States (Bekker et al., 2005), South Africa (Polteau et al., 2006), Fennoscandia (Marmo and Ojakangas, 1984; Strand and Laajoki, 1993), West Australia (Martin, 1999), South America (Bekker et al., 2003), India (Hambrey and Harland, 1981), and most recently, China (Chen et al., 2019).

2.1 Regional Geology

The sedimentary rock composing the Huronian Supergroup forms a southward thickening assemblage deposited first in rift basins, then in a more laterally extensive passive margin environment (Figure 2) (Van Schmus, 1976; Fralick and Miall, 1981; Fralick, 1984, 1985; Miall, 1985; Young and Nesbitt, 1985; Fralick and Miall, 1989; Young et al., 2001; Bennett, 2006; Young, 2013a; Hoffman, 2013). The succession begins at 2.49 to 2.44 Ga (Van Schmus, 1965; Krough et al., 1984) with rift volcanics (2.45 Ga Ketchum et al., 2013) overlying alluvial fans of the Livingston Creek Formation (Bennett, 2006). These units, though in places over a kilometer thick, are only sporadically present. The much more laterally continuous glacial outwash sandstones (Fralick and Miall, 1987) of the Matinenda Formation blanket the underlying Formations and Archean basement (Fralick and Miall, 1989). Advancing glacial ice scoured the lose sands and uraniferous conglomerates of the Matinenda Formation incorporating this material into the diamictites of the Ramsay Lake Formation. The ice advanced from what is today the north, but probably did not extend to all areas along the southern margin of the basin (Fralick and Miall, 1989). This calls into question the assertion that the Makganyene glaciation of South Africa, a between 2442 Ma and 2435 Ma correlative unit to the Ramsay Lake Formation (Gumsley et al., 2017), was a snowball event. Isostatic loading had caused subsidence prior to arrival of the ice sheet and open water marine conditions resumed after ice melt back (Fralick and Miall, 1989). This transitioned into prodelta to distributary mouth bar deposits of the upper Pecors and lower Mississigi Formations, which in turn is overlain by sandy braided fluvial deposits (Long, 1978) of the middle to upper Mississigi Formation. The Bruce ice sheet advanced over this sand plain, with accompanying isostatic load induced subsidence and development of floating ice (Frarey and Roscoe, 1971; Parviainen, 1973; Bennet et al., 1991). With deterioration of the ice shelf the rainout diamictites were overlain by a thin siltstone layer,

which appears to be loess similar to the loess overlying the Ramsay Lake diamictites (Fralick and Miall, 1989). Parallel laminated limestones, siltstones and silty limestones of the Espanola Formation sharply overlie either the thin siltstone or the diamictite. Its thickness is variable, but generally greater than 200 meters. The upper contact is gradational, as the Espanola becomes interlayered with marine sandstones of the Serpent Formation. Both are eroded, quite extensively in places, by the first Gowganda Formation ice advance. Again isostatic loading caused flooding associated with this glaciation and upon melt-back coarsening upward deltaic deposits were laid down (Junnila and Young, 1995) only to be overridden by the second, more limited, Gowganda glaciation (Beh, 2012; Hoffman, 2013). This was the last Huronian ice sheet and upon its retreat a coarsening upward succession was overlain by sands of the Lorrain Formation, which in turn was overlain by near-shore to tidal mudflat sediments of the Gordon Lake Formation. Redbeds first appear in the Gowganda interglacial deposits and become abundant in the Gordon Lake Formation (Bennett, 2006). A 2.31 Ga U-Pb zircon age comes from tuffaceous beds in the Gordon Lake Formation (Rasmussen et al., 2013). The uppermost unit in the succession consists of the near-shore sandstones forming the Bar River Formation.

3.1 Methodology

Fieldwork was conducted during the summers of 2016 and 2017 examining outcrops of the Espanola Formation in the study area (Figure 1) and logging core from drill holes 150-1, 150-2 and 144-1 drilled near Elliot Lake and stored at the Ontario Ministry of Natural Resources and Mines, Sault Ste. Marie. Over 100 samples were collected from outcrop and drill core, and after

petrographic examination 60 were selected for inductively coupled plasma – atomic emission spectroscopy (ICP-AES) and inductively coupled plasma – mass spectrometry (ICP-MS) analysis, 78 for stable isotope analysis and 8 for Sr and Nd isotope analyses.

Samples destined for ICP-AES and ICP-MS analyses were crushed in an agate mill and 0.2g of each was subjected to a one hour pre-leach in 5% acidic acid. This fluid was discarded and the carbonate fraction was separated during a 24 hour partially digestion using 5% acetic acid. ICP-AES analyses were conducted using a Varian Vista Pro Radial atomic emission spectrometer, and ICP-MS analyses were performed on a Perkin-Elmer Elan DRC-e quadrapole mass spectrometer at the Lakehead University Instrumentation Laboratory. A blank was inserted for every 10 samples and two carbonate standards were run for approximately every 25 samples. The analytical accuracy of reported results is ±10% for ICP-AES and ±5% for ICP-MS.

Stable isotopes of carbon and oxygen were measured at the European Institute for Marine Studies, Pôle Spectométrie Océan, in Brest. The powdered samples were placed in a Kiel IV where concentrated H_3PO_4 was added and allowed to react at 72^{O} C. Samples were analyzed with a Finnigan MAT 253. Results are reposted against the Vienna Pee Dee belemnite (V-PDB) standard with an analytical error (2σ) of 0.2‰ for $\delta^{18}O$ and 0.1‰ for $\delta^{13}C_{carb}$.

Isotopes of Sr and Nd were analyzed on a Finnigan MAT 262V at Memorial University of Newfoundland's Earth Resource Research and Analysis Facility after a partial 5% acetic acid leach of carbonate from a mixture of carbonate/siliclastic material. Following overnight partial digestion samples were centrifuged for 5 minutes and the solutions were pipetted into Savilex©

Teflon capsules and dried overnight. Samples were then dissolved in 1ml of double distilled 8N nitric acid and 0.5 ml of each sample was loaded onto columns containing pre-cleaned Sr Spec resin. Rb and other elements were washed away using 8M and 3M nitric acid. The final Sr separate was collected in 2 ml of double distilled water. For Nd after samples underwent a 5% acetic acid leach they were centrifuged for 5 minutes and the solution was pipetted into a Savilex© Teflon capsule and dried overnight. Samples were then taken back up in 5ml of 6M HCl and left on a hotplate for 4-5 days before being dried down overnight. The residual siliclastic material in the tubes was then dried and weighed to determine the exact amount of carbonate leached from the sample. 0.5-1 ml of 2.5 M HCl was added to each dried sample as well as the required amount of a mixed $^{150}Nd/^{149}Sm$ spike. Samples were then loaded into a column containing cation exchange resin AG-50W-X8, H+ form, 200-400 mesh. A bulk REE solution was collected and dried overnight. Samples were taken up in 0.18M HCl and loaded on a second column containing Eichrom© Ln resin (50-100 mesh) to isolate Sm and Nd separately from the other REES. All reagents were purified in order to ensure a low contamination level. Sm and Nd concentrations and the Nd and Sr isotopic compositions were determined using a multi-collector Finnigan Mat 262 mass spectrometer in static mode for concentration determination, and dynamic mode for isotopic composition determination. Sm and Nd were loaded separately onto double rhenium filament assemblies while Sr utilized a single tungsten filament with 1 microlitre of Sr activator (Tantalum fluoride). Instrumental mass fractionation of Sm, Nd and Sr isotopes are corrected using a Raleigh law relative to $^{146}Nd/^{144}Nd = 0.7219$, $^{152}Sm/^{147}Sm = 1.783$ and $^{88}Sr/^{86}Sr = 8.375209$. The reported $^{143}Nd/^{144}Nd$ and $^{87}Sr/^{86}Sr$ ratios are corrected for the deviation from repeated duplicates of JNdi-1 ($^{143}Nd/^{144}Nd = 0.512115$, Tanaka et al., 2000) and NBS 987 ($^{87}Sr/^{86}Sr = 0.710240$, Veizer et al., 1999) standards. Replicates of the

standards give a mean value of $^{143}Nd/^{144}Nd = 0.512095 \pm 9$ (1SD, n=20) for JNdi-1 and $^{87}Sr/^{86}Sr = 0.710234 \pm 9$ (1SD, n=20) for NBS 987.

4.1 Sedimentology

The Espanola Formation, has been broadly defined as being composed of three major members and a local fourth member that is developed in some of the southernmost exposures (Quirke, 1917; Collins, 1925; Robertson, 1964; Young, 1973; Card et al., 1977; Bernstien and Young, 1990; Long, 2009). The three major members of the Espanola Formation are defined by their dominant lithologies, resulting in the subdivision of a lower limestone unit, a middle siltstone unit, and an upper heterolithic or dolostone member (Quirke, 1917; Collins, 1925; Robertson, 1964; Young, 1973; Card et al., 1977; Bernstien and Young, 1990). A sandstone-rich member constitutes the local fourth member, and is developed in outcrops in the southern area where it overlies the middle siltstone member (Frarey and Roscoe, 1970). Thickness of the formation is highly variable, with each individual member ranging from 15m to ~300m, but there is a general trend of southward thickening of the entire formation due to an increase in the thickness of the siltstone member and the presence of the additional sandstone member (Meyn, 1970; Young, 1973; Eggertson, 1975; Card et al., 1977).

The Espanola Formation is unique within the Huronian stratigraphy because of its carbonate-content, which is ubiquitous throughout the formation but is highly variable in its proportion of the total rock composition (Frarey and Roscoe, 1971; Young, 1973; Bernstien and Young, 1990; Bekker et al., 2005). Proportions of carbonate in the Espanola Formation range from 10-90%,

with the lower limestone member having the highest concentration of carbonate minerals, averaging 30%, while the other three members have carbonate concentrations ranging from 10-20% (Card et al., 1977; McLennan et al., 1979). The ratio of calcite to dolomite is also variable across all three members and both the limestone and dolostone members contain calcite as the dominant carbonate mineral, while the siltstone member contains equal proportions of both calcite and dolomite (Card et al., 1977).

Glacial diamictites of the Bruce Formation (Figure 3A) contain, in their upper portion, an area of interlaminated siltstones and carbonate with dropstones (Figure 3B). The diamictites are sharply overlain in most locations by a thin layer of well-sorted siltstone (Figure 3C). This is overlain in turn by the lower portion of the Espanola Formation, which is dominated by interlaminated limestone and siltstone, with individual layers varying from mm-scale to 2 cm (Figure 3D). Thicker carbonate layers, ranging from 2 to 10 cm, are also sporadically present. Layering is contorted in places and may grade into slump breccias consisting of white carbonate clasts in a grey siliciclastic dominated matrix.

There is a gradational contact with overlying siltstones and fine-grained sandstones consisting of an upward decrease in carbonate and an increase in the average coarseness of the siliciclastics. Thinly layered, fine-grained sandstones and siltstones are parallel laminated or massive and commonly graded. Wavy to lenticular bedding is also common and in places spatially associated with contorted and slumped areas. Calcareous layers and cements are ubiquitous throughout this unit.

The middle and upper portions of the stratigraphy in the northern outcrop areas is dominated by a highly variable assemblage of lithofacies that readily changes character. The most common lithologies are siltstone and calcareous siltstone, with variable amounts of carbonate, sandstone and mudstone, which are massive or parallel laminated, or ripple laminated, or hummocky cross-stratified, and may be normally graded. Desiccation cracks are rare, but present. Soft sediment deformation, including loading, dewatering structures and contorted bedding are common, as are intraformational flat pebble conglomerates; some obviously formed during water escape. Ferruginous carbonate interbeds are also present in this assemblage (Figure 3E,F). Rare chert layers are present in the ferruginous dolomite beds, and, in places, elongate chert clasts are diffusely scattered in them. Parallel to ripple laminated white carbonate beds are also rarely present directly below the ferruginous ones. Sedimentary structures in the ferruginous carbonate are similar to the siliciclastic units they interlayer with.

In the extreme southern outcrop area the middle and upper Espanola Formation is interlayered with fine- to medium-grained, cross-stratified sandstone, siltstone and calcareous sandy siltstone. Bedforms are, in order of declining abundance: trough cross-stratification, parallel lamination, planar cross-stratification, massive layer, hummocky cross-stratification, and ripple lamination. This lithofacies association is transitional into the cross-stratified sandstones of the Serpent Formation.

The lithofacies associations described above are commonly intruded by intraformational breccias with sharp contacts. Clasts are dominated by siltstone, but also consist of other typical Espanola lithologies.

Past interpretations of Espanola sedimentology involved a transgression followed by a subsequent regression during the Bruce glacial recession (Robertson, 1964, 1968; Parvianien, 1973; Young, 1973, Bernstien and Young, 1990). The lower limestone member was commonly suggested to have been deposited in a subtidal environment under relatively low energy conditions (Young, 1973; Eggertson, 1975; Bernstien and Young, 1990) with the predominance of carbonate with lesser siltstone and shale partings suggesting that clastic input was minimal (Young, 1973; Eggertson, 1975). The source of these laminations has been interpreted to be seasonal in origin, or through influxes of sediment via storm-derived currents or turbidity currents (Robertson, 1964; Bernstien and Young, 1990). The overlying Siltstone Member was also interpreted to have been deposited in deep water, deeper even than in the underlying Limestone Member, and depositional processes were suggested to be largely similar to the underlying Limestone Member and differing merely in the carbonate content (Collins, 1925; Young, 1973; Eggertson, 1975; Bernstien and Young, 1990). The upper Dolostone Member was generally accepted to represent a higher energy environment (Bernstien and Young, 1990).

The lack of features suggesting the influence of traction currents or erosive scouring in the interlayered carbonate and siltstone, the lowest unit in the Espanola, indicates deposition in a quiet water environment by suspension settling (cf. Orton and Reading, 1993). The siliciclastic sediments may have been delivered as individual buoyant plumes carrying silt sourced from river mouths, or this fine-grained material may have been delivered to the water's surface as wind-blown loess. The carbonate would represent precipitation in the water column and concentration on the bottom during hiatuses between silt deliveries during storm events. Slumping of these

units would have been facilitated by post-glacial topographic relief, fluctuating sedimentation rates and tremors due to isostatic adjustments. Increasing delivery of fine-grained siliciclastics caused a decrease in the carbonate content of the depositional system. The preponderance of thin, graded layers in this portion of the section is typical of storm-derived sediment plumes moving offshore (Smith and Hopkins, 1972; Aigner and Reineck, 1982; Nittrouer and Wright, 1994). These deposits are transitional into the higher energy environment of the nearshore (Young, 1973; Eggertson, 1975) with fair-weather wave ripples (Komer, 1976; Bourgeois and Leitholl, 1989) and storm induced geostrophic flow producing hummocky cross-stratification and upper flow regime parallel lamination (cf., Leckie and Walker, 1982; Plint, 2010; Bayet-Goll et al., 2014). Occasional sub-aerial exposure formed desiccation cracks and fenestrae in intertidal carbonates (Bekker et al., 2005). Hummocky cross-stratified ferruginous carbonate represents storm reworking of fair-weather, suspension deposited carbonate. Intraformational flat pebble conglomerate beds in ancient successions, like the ones present in the ferruginous carbonate, can be interpreted to have formed below fair-weather wave base (Kazmierczak and Goldring, 1978; Markello and Read, 1982; Sepkoski, 1982; Demicco, 1983; Wilson, 1985; Grotzinger, 1986; Lee and Kim, 1992; Mount and Kidder, 1993), though some may represent storm deposits on the shore-face and tidal flats (cf. Myrow et al., 2004). Accumulations of trough cross-stratified sandstone were probably deposited in the near-shore (Young, 1973; Bernstien and Young, 1990) as distributary mouth bars near sediment entry points.

The entire record from offshore, below storm wave-base, fine-grained carbonates and siliciclastics, deposited immediately post-glacial, to offshore, above storm wave-base hummocky cross-stratified sandstones and grainstones, and finally to strand-line microbial carbonates

(Hofmann et al., 1980) and nearshore sandstones is present in this succession. These form a coarsening and thickening upward assemblage over hundreds of meters. Nearshore lithologies consisting of a mixture of bedding types are more prevalent in the north, with the major sediment entry point probably located to the northeast. Isostatic triggered slumping was common. Minor relative sea-level fluctuations are recorded in the northern portion of the area by intervals of desiccation followed by reflooding.

5.1 Geochemistry

5.1.1 Isotope Geochemistry

Stable isotopic analysis of the Espanola Formation was previously conducted on some of the drill cores and field outcrops of the Espanola Formation (Bekker et al., 2005). They uncovered several interesting pieces of information, including the presence of consistent negative $\delta^{13}C$ values, a feature that is also recognized from Neoproterozoic cap carbonates (Veizer et al., 1992; Bekker et al., 2001; Bekker et al., 2005). Oxygen in Espanola carbonates is also depleted in $\delta^{18}O$, which has been suggested to be the result of interaction with hot fluids (Bekker et al., 2005). A lack of correlation between $\delta^{13}C_{carb}$ and $\delta^{18}O$ is therefore used to suggest that the depleted $\delta^{13}C$ values observed within the Espanola carbonates are of a primary origin and reflective of anomalous water chemistry (Bekker et al., 2005).

Our stable isotope analysis of the Espanola Formation carbonates revealed the presence of a highly negative $\delta^{13}C_{carb}$ excursion at the top of the Bruce Formation in drill-hole E150-2. Values collected from a laterally limited laminated dropstone facies (Figure 3B) are extremely low at

approximately -10‰ for $\delta^{13}C_{carb}$ (Figure 4). Associated $\delta^{18}O$ are also more negative than the values that are typical for the remainder of the samples, but the magnitude of the excursion is not as stark as that of the $\delta^{13}C_{carb}$ values (Figure 4). While anomalous $\delta^{13}C_{carb}$ values were recognized from Espanola Formation carbonates, the extreme negative $\delta^{13}C$ anomaly preserved within laminated carbonate and siltstone with drop-stones present for 12 m interlayered with the top of the Bruce Formation in drill hole E150-2 suggests that the water mass that deposited these carbonates was unique.

Omitting the very negative data points from drill hole E150-2, the remainder of the Espanola carbonate samples have $\delta^{13}C_{carb}$ ranging from -4.9‰ to -1.3‰. Additionally, drill-hole E150-2 has a systematic upwards trend of increasing $\delta^{13}C_{carb}$ from ~-4‰ to -2.5‰ (Figure 4). These values are consistent and fall within the range of -4.0‰ to -0.8‰ of previously collected data from a different drill hole by Bekker et al. (2005), and are overall slightly more negative on average than data presented by Veizer et al. (1992), who analyzed samples from the lower member of the Espanola Formation and produced values with a range of -1.3+/-0.7‰. Thus, a negative $\delta^{13}C_{carb}$ signal for the carbonates of the Espanola Formation appears to be consistent across the lateral continuity of its exposure, as well as throughout its stratigraphy. A negative $\delta^{13}C_{carb}$ signal has also been produced for samples analyzed from carbonate of the Snowy Pass Supergroup that overlie the second of three glacial horizons, which is believed to represent an equivalent carbonate-bearing formation to the Espanola (Bekker and Karhu, 1996; Bekker et al., 1999, 2001).

Eight samples from drill-hole E150-2 were selected for strontium isotope geochemistry. The samples are all extremely radiogenic with $^{87}Sr/^{86}$ Sr values ranging from 0.75836 to .73702 (Figure 5). The ε(0)Nd values for the same eight samples vary from -26.3 to +3.9 (Figure 5). In both cases the more extreme values are from the interlaminated carbonate and siltstone with drop-stones in the uppermost Bruce Formation: the same unit that has the very light C_{carb} isotopes and most radiogenic Sr.

5.1.2 Rare Earth Elements

It was necessary to perform partial digestions on samples collected from the Espanola Formation to isolate the REE pattern preserved within the carbonate from the high siliciclastic component of many samples. Numerous studies have suggested that carbonates precipitated from a body of water will preserve information about the chemistry of the water (e.g., references in Fralick and Riding, 2015). This information may be preserved within the REE concentrations, as these elements largely behave in a similar manner, with some exceptions, and undergo little alteration in their relative abundances during sedimentary processes (McLennan et al., 1980, 1983, 2003; McLennan, 1989). The exceptional behavior of certain rare earth elements allows for the interpretation of some aspects of water chemistry in which the precipitates had formed. These include Y/Ho fractionation and shape of the REE pattern when normalized to post Archean Australian shale (PAAS, Taylor and McLennan, 1985).

Terrigenous materials have a constant chondritic Y/Ho weight ratio of ~28, but seawater values have ranged from ~44 to 74 in the past, indicating fractionation processes influence the ratio (Nagarajan et al., 2011). Environmental interpretations based on the Y/Ho ratio of a precipitate

are made possible by the behavioral differences between Y and Ho in the subaqueous setting (Kawabe et al., 1991), differences that result in an enrichment of Y compared to Ho in seawater (Nozaki et al., 1997). Several mechanisms for the fractionation of Y and Ho have been suggested, such as weathering processes and differing solution complexation and solubilities with phosphates (Bau et al., 1995; Nozaki et al., 1997). The most probable reason for the observed fractionation trends is due to a deviation in completive reactions and scavenging of Y compared to Ho and other REEs (Nozaki et al., 1997). While Y and Ho have similar ionic radii, Y behaves differently from Ho in solution because of the thermochemical effects of the presence or absence of 4f electrons (Kawabe et al., 1991; Nozaki et al., 1997). Scavenging by particulate matter and fractionation of Y and Ho occurs in the weathering environment and throughout the element's travel through rivers, estuaries and into the ocean (Nozaki et al., 1997). Modern seawater has an average Y/Ho weight ratio of ~54 (Nagarajan et al., 2011), whereas Espanola Formation carbonates have Y/Ho weight ratios with an average superchondritic value of ~35. However, there is a large range and variability of Y/Ho ratios, with values from ~20 to 50 (Figure 6).

The shape of PAAS normalized REE patterns vary with lithofacies association and also somewhat within lithofacies associations. The calcite in the dropstone-bearing interlaminated carbonate and siltstone in the uppermost Bruce Formation has, in addition to very negative $\delta^{13}C$ values, distinctive REE patterns (Figure 4). These patterns are characterized by flat light REEs, consistent negative Eu anomalies, and heavy REEs that range from negatively to positively sloped. A limited number of other samples have similar REE patterns to these. One is in drill-hole 150-1 6 m above the Bruce diamictite. Four others were from outcrops of the interlaminated

carbonate and siltstone without dropstones with unknown stratigraphic positions. Moving slightly up stratigraphy, samples collected from the interlaminated carbonate and siltstone in drill hole 144-1, directly above the contact with the Bruce Formation, undergo a progressive upward change in REE pattern, from flat and shale-like, to a 'hat-like', middle REE enriched pattern (Figure 7). Overlying carbonates forming the bulk of the interlayered carbonate and siltstone unit have very consistent features, with relatively depleted light REEs (Figure 4). Heavy REEs are typically flat but may be slightly positively-sloped. Two outlier samples, one of which is located within the laminated dropstone unit, have similar light depleted REE patterns, but are different in that they have slightly negatively sloped heavy REEs (Figure 4). Samples from ferruginous and associated white carbonate layers in the northern outcrop area have the characteristic light REE depletion along with slight heavy REE depletion (Figure 8). Most importantly they are the only layers to have positive Eu anomalies.

5.1.3 Barium

Within the interlaminated carbonate and siltstone unit in drill hole E150-1 there is a Ba-rich horizon located between 8 and 9.5 m above the contact with Bruce diamictites (Figure 9). Partial digestion values are near 10 ppm for samples immediately below and above this area, but in this zone they range up to 3600 ppm. The REE patterns for three of the samples massively enriched in Ba have large positive Eu anomalies, though these are difficult to evaluate due to BaO interference with measuring Eu. Organic $\delta^{13}C$ values from the same set of samples show a slight decreasing trend in values from approximately -25‰ below the Ba enriched unit to - 27.5‰ in the Ba enriched unit.

6.1 Discussion of Geochemistry

6.1.1 The Basal Espanola Formation

The stratigraphically lowest carbonate unit consists of the interlayered carbonate and siltstone with dropstones that forms a 9.5 m thick succession in the diamictite and sandstone of the uppermost Bruce Formation. These carbonates contain very negative $\delta^{13}C$ values (Figure 4) that are close to those recorded from the Wonoka-Shuram anomaly, the most extreme negative carbon isotope anomaly associated with the Neoproterozoic glacial cycles (Halverson et al., 2005). The Wonoka-Shuram anomaly records $\delta^{13}C_{carb}$ as low as ~-11‰ and has a unique association with the rise of metazoan life (Halverson et al., 2005; Grotzinger et al., 2011). This provides an interesting comparison to the Bruce glacial event and the Espanola Formation, which are hypothesized to be directly correlated to global changes involving a rise in atmospheric oxygen (Sekine et al., 2011; Hoffman, 2013). Several hypotheses have been put forth to explain the Wonoka-Shuram anomaly, including; 'Snowball Earth' and CO_2 build-up (Hoffman et al., 1998), methane release (Kennedy et al., 2001), oxidation of dissolved organic matter (Rothman et al., 2003), weathering of fossil organic matter (Kaufman et al., 2007), and upwelling of ^{13}C-depleted deep oceanic waters (Williams and Schmidt, 2018). The similarities in values obtained from carbonates in the laminated dropstone unit in the upper Bruce Formation in drill hole E150-2 may suggest that comparable processes to the driving mechanism for development of the extremely negative $\delta^{13}C$ Wonoka-Shuram anomaly were ongoing during its deposition. It is interesting to note that the correlative Paleoproterozoic Sausar Group in India has a peak negative excursion of -7.4‰ V-PDB (Mohanty et al., 2015), which is close to the range of some of the highly negative values collected from the laminated dropstone facies.

The Paleoproterozoic Sausar Group in India also preserves negative Eu anomalies in its rare earth element patterns similar to samples from the interlayered carbonate and siltstone with dropstones, and in some locations the interlaminated carbonate and siltstone without dropstones, occurring in the lower stratigraphy of the Espanola Formation. These unusual patterns (Figure 4) are similar to dolomites associated with mineralization in the Zambian Copperbelt (Roberts et al., 2009) and carbonate-rich shales of the Kupferschiefer (Sawlowicz, 2013). Carbonates associated with mineralized zones in the Copperbelt also have very negative $\delta^{13}C$ values, which Selley et al. (2005) believed were caused by recycling of carbon freed by the oxidation of organic carbon. The Copperbelt also has extremely radiogenic $^{87}Sr/^{86}Sr$, varying between 0.71114 and 0.74688 (Roberts et al., 2009). The similarity of REE patterns with Eu depletion, very negative $\delta^{13}C_{carb}$ values (Figure 4), and extremely radiogenic $^{87}Sr/^{86}Sr$ ratios (Figure 5) for some samples of carbonate from the Zambian Copperbelt and carbonate with dropstones in the Espanola Formation is striking. These features in the Copperbelt are believed to have formed diagenetically from basinal fluids that interacted with methane and bicarbonate produced by the oxidation of organic carbon (Roberts et al., 2009). REE patterns with depleted Eu in carbonates from the Kupferschiefer are thought to be caused by the Eh that prevailed during sedimentation and/or diagenesis, with the negative Eu anomalies related to more highly reducing conditions (Sawlowitz, 2013). This occurs when Eu^{3+} comes into contact with highly reducing fluids and is reduced to more soluble Eu^{2+} (MacRae et al., 1992; Sawlowicz, 2013). The highly reducing conditions produced by degradation of organic matter, methanogenises and/or methane release during destabilization of gas clathrates would produce conditions favourable for the fractionation of Eu and could produce fluids with a relative deficiency in Eu compared to the other REEs.

Methane seepage has been proposed to have influenced deposition of some Neoproterozoic cap carbonates (cf. Kennedy et al., 2001; Wang et al., 2008). Furthermore, not only would methane seepage influence dissolved REEs in sub-surface sediments and bottom waters, it would also directly cause the precipitation of authigenic carbonates in those environments and could be a strong driving mechanism for precipitation of the carbonate fraction of some of the Espanola Formation (cf., Aloisi et al., 2002; Bayon et al., 2013; Lemaitre et al., 2014). In addition the positive Gd anomalies in the Kupferschiefer and Bruce Formation carbonates may have developed due to release into the fluid phase during diagenesis of Gd concentrated in the humic acids of the organic matter (e.g. Kautenburger et al., 2014).

Methane seepage may also be the source of the highly negative $\delta^{13}C_{carb}$ signature in the carbonate with dropstones (Figure 4); similar to what has been suggested as the cause of the negative $\delta^{13}C_{carb}$ in Neoproterozoic cap carbonates (Kennedy et al., 2001; Jiang et al., 2003; Wang et al., 2008). One of the major complications to this hypothesis, as in discussions of the Neoproterozoic cap carbonates, is the lack of an associated methane-derived $\delta^{13}C$ signature (e.g. Shields, 2005; Corsetti and Lorentz, 2006). However, there have been investigations of the Neoproterozoic Doushantuo cap carbonate that have identified unequivocal evidence for methane seeps in the form of negative $\delta^{13}C_{carb}$ values as low as -48‰ (Jiang et al., 2003; Wang et al., 2008). No definitive methane seep signature was identified in the Bruce or Espanola Formations. However, alternative explanations that have been provided to explain the typical lack of these signatures in Neoproterozoic cap carbonates may apply, i.e. the methane seep signature was diluted by ambient seawater during precipitation of carbonate and homogenization during diagenesis (Jiang

et al., 2003, 2006a, 2006b). Alternatively or also, the oxidation of organic carbon may have provided light carbon and reducing conditions.

Giddings and Wallace (2009) found that the most negative values in the Neoproterozoic Umberatana Group cap carbonate occur in the basinal facies, with values ranging from -6.7‰ to -3.7‰. The most negative values of the Espanola Formation, in the laminated dropstone facies, are also in a deeper shelf environment of deposition. The inferred mechanism for the depth-dependent factor on $\delta^{13}C_{carb}$ in the Umberatana Group cap carbonate is suggested to be a result of stratification, wherein organically-derived carbon accumulates in deep water before destratification, and upwelling of the $\delta^{13}C$-depleted waters occurs in the aftermath of the glacial event (Giddings and Wallace, 2009). The idea of basinal water stratification is appealing as the fluids would be capable of producing isotopically light carbon as cements in the silt-rich layers and precipitating carbonate layers with a similar isotopic composition from the stratified bottom water.

The carbonate with dropstones has very negative εNd(0) values as low as -26 (Figure 5). This contrasts with the carbonate without dropstones above the Bruce Formation which averages -0.5 εNd(0) (Figure 5). A very similar trend is present in the Holocene carbonates from cored pelagic sediments in the northern northeast Atlantic Ocean (Blaser et al., 2019). There two layers of ice rafted debris correspond to Heinrich Stadials, cold events during late continental glaciation. These two layers have εNd as low as -28 and -24, whereas pelagic sediment without ice rafted debris deposited during the glacial maximum have values of -9, and late Holocene sediments at the top of core have -12. Blaser et al. (2019) believed low oxygen, reducing conditions

developed in the iceberg rafted debris layers resulting in Nd liberated into the pore waters. Authigenic dolomite cements precipitating from the pore waters incorporated the REEs released from detritus that had been supplied by the Laurentide ice sheet from the Canadian Shield (Blaser et al., 2019). Considering the source of the sediment was, in general, very similar for the ice rafted debris in the Holocene Heinrich Stadial layers and the uppermost Bruce glacial deposits and their εNd values are virtually identical it's reasonable to assume that the processes which produced those values were similar. This is reinforced by a TDM model age of 2755 my from carbonate in the Espanola ice rafted debris, a typical average for the Archean portion of Superior craton, indicating REE exchange has taken place between that debris and the carbonate. A difference does exist in that the Bruce dropstone deposits in addition to containing authigenic dolomite cements also have carbonate layers that precipitated on the seafloor from bottom waters. In the northern Atlantic example there was very little vertical mobility of Nd, and insignificant amounts reached the overlying water mass (Blaser et al., 2019). Studies of more shore proximal late Holocene sediments indicate in these locations Nd is released from siliciclastic sediment into the water column (Abbott et al., 2015) altering the εNd values of the water (Grasse et al., 2017; Yu et al., 2017) and, potentially, precipitates from it.

The barium-rich unit 8 to 9.5 meters above the Bruce Formation is stratigraphically close to the underlying ice rafted, debris-rich carbonates (Figure 9). It forms a small portion of the carbonates interlayered with siltstone that do not contain ice rafted debris and were deposited below wave base. Most of this deep water unit is calcite except in and near the barium-rich horizon where it is ferronian dolomite. Barite horizons in Neoproterozoic cap carbonate successions (Hoffman and Schrag, 2002; Jiang et al., 2003; Shields et al., 2007) occur at the

contact between underlying dolomitic and overlying calcitic units, which suggests that they mark a shift from a sulfate-poor to sulfate-rich marine environment, due to the known inhibiting effect of sulfate ions on the precipitation of dolomite (Baker and Kastner, 1981; Shields, 2005; Shields et al., 2007). However, here the opposite occurs with the barite associated with dolomite in a mostly calcite succession. . While the stratigraphic control on the Ba-rich horizon is not as clear in the Espanola Formation as in Neoproterozoic cap carbonates, nor as laterally extensive, it is interesting that it occurs within a few meters of the contact with the underlying Bruce diamictite, and roughly within or close to the same stratigraphic horizons which host negative Eu anomalies and low $\delta^{13}C_{carb}$. These features are possibly the result of methane seepage (e.g. Shields et al., 2007), or a build-up of HCO_3^- formed from oxidized organic material, and similarly, a Neoproterozoic cap carbonate in China preserves barite in association with light $\delta^{13}C$, evidence of methane seepage (Jiang et al., 2003). The small and isolated occurrence of the Ba-rich horizon suggests that whatever the source of the fluids, the conditions that allowed for deposition of the barite were short-lived and isolated.

6.1.2 The Middle Espanola Formation

The $\delta^{13}C_{carb}$ values in the Espanola carbonate directly overlying the glacial rocks in drill hole E150-2 rapidly increase from -4.5‰ to -2‰, then 88 m higher (50 m minus intrusive breccias) decrease to -4‰. The increase from -10 in the uppermost Bruce Formation to -4.5 immediately above the Bruce Formation is accompanied by a drastic change in REE patterns from Eu and mostly HREE depleted patterns to the smooth LREE depleted patterns of the overlying carbonate (Figure 4). It is likely reducing conditions in the substrate that produced diagenetic leaching of the siliciclastics into pore waters and overlying bottom waters of a stratified water column, was

replaced by an unstratified system more open to ocean water (e.g. Giddings and Wallace, 2009). This transition is also shown by the upward progression from relatively flat REE patterns 2 m above the Bruce to the typical smooth, LREE depleted pattern 20 m higher (Figure 7). The PAAS normalized flat REE patterns of the carbonate reflect derivation of those elements from the siliciclastic component, whereas the light depleted patterns have more in common with typical patterns for both Precambrian and more modern seawater. The heavier -2‰ values transition up-section to values of-4‰, probably indicating less seawater influence. During deglaciation shoreline position and water depth are determined by the opposing effects of isostatic rebound and absolute sea-level rise driven by melting ice. Fluctuations in these rates would be expected to cause changes in the hydrodynamic circulation on the shelf. It is possible that this resulted in rapid deepening during early deglaciation as ice shelves disintegrated, and development of a basal wedge of marine water. This would cause the $\delta^{13}C$ to increase to -2‰. With time isostatic rebound would outstrip absolute sealevel rise shallowing the area (e.g. Nutz et al., 2015; Dietrich et al., 2017; and references therein) and forcing the marine wedge seaward, decreasing the $\delta^{13}C$ to -4‰.

From there to the top of the hole, a distance of 160 m, there is a systematic upwards trend of increasing $\delta^{13}C_{carb}$ from ~-4‰ to -2.5‰. A similar pattern was produced by systematic sampling of drill hole E150-1 by Bekker et al. (2005, Figure 4), where a general upwards trend of increasing $\delta^{13}C_{carb}$ occurs through the upper stratigraphy of the Espanola Formation. Thus, a negative $\delta^{13}C$ signal for the carbonates of the Espanola Formation appears to be consistent across the lateral continuity of its exposure (Bekker et al., 2005), as well as throughout its stratigraphy. A negative $\delta^{13}C$ signal has also been produced from samples analyzed from carbonate of the

Snowy Pass Supergroup that overlie the second of three glacial horizons, which is believed to represent an equivalent carbonate-bearing formation to the Espanola (Bekker and Karhu, 1996; Bekker et al., 1999, 2001). The consistency in stratigraphy and carbon isotopic composition between these two formations suggests that the signal was not produced by a local environment, but instead may have global implications (Bekker et al., 2005). Furthermore, the identification of the stratigraphic trend of increasing $\delta^{13}C$ in drill holes E150-2 and E150-1 (Bekker et al., 2005, Figure 4) further supports an argument that the $\delta^{13}C$ of the Espanola carbonates is primarily controlled by a decaying meltwater signature (cf. Yoshioka et al., 2003; Liu et al., 2014, 2018; Wen et al., 2015; Caxito et al., 2018; Wei et al., 2019).

Both the occurrence of highly negative $\delta^{13}C$ at the base of cap carbonates, and the upwards increase in values of $\delta^{13}C$ through stratigraphy has also been reported from Sturtian glaciations, and is a typical feature of Neoproterozoic cap carbonates in general (Kennedy et al., 1998; Halverson et al., 2005, 2010). One interpretation of $\delta^{13}C$ patterns observed in the Umberatana Group in South Australia, is that the variation is facies influenced, with deeper water facies producing values ranging from –5.5‰ to –3.5‰, and shallower water facies ranging from –3.6‰ to –0.3‰ (Giddings and Wallace, 2009). This work has been supported by observations of other cap carbonates (de Alvarenga et al., 2004; Shen et al., 2005; Rieu et al., 2006; Kasemann et al., 2010). This may be the result of isostatic rebound dominating over absolute sealevel rise during early deglaciation (e.g. Nutz et al., 2015; Dietrich et al., 2017) resulting in a shallowing trend and less freshwater influx with terminal disintegration of the ice sheet.

The εNd values for the interlayered carbonate and siltstone section of drill-hole H150-2 provide an interesting contrast to the underlying dropstone bearing layers. The underlying layers were compared to iceberg rafted sediments in the northeast Atlantic Ocean (Blaser et al., 2019) to investigate whether the source of the εNd in both deposits was sediment from the Canadian Shield. Therefore εNd(0) was used (Figure 5) as the time span from the average age of the rocks in the Shield till now was the variable being compared. If the εNd(0) in the Espanola dropstone bearing unit is the same as the Holocene iceberg rafted sediments, which it is, this means that Nd was derived from the sediment, similar to the Holocene iceberg rafted debris (Blaser et al., 2019). However, the εNd(0) values of -9 to -12 for Holocene sediment without iceberg rafted material above the iceberg rafted zones reflects incorporation of Nd into precipitating carbonate from seawater (Blaser et al., 2019). To compare the Espanola Formation εNd values with this data the εNd value at 2400 my must be used as that is approximately when precipitation from seawater would have occurred. The εNd(2400) values for Espanola interlayered carbonate and siltstone above the ice rafted debris zone ranges from -8 to -12 εNd(2400) (Figure 5), which by comparison to the Holocene data (Blaser et al., 2019), strongly indicates a significant Paleoproterozoic seawater source. There is also a large decrease in the $^{87}Sr/^{86}Sr$ ratio moving up section from the iceberg rafted debris zone to the overlying sediment without dropstones (Figure 5). Derivation of radiogenic Sr in the siliciclastic fraction over time would lead to some incorporation of it into the carbonate fraction where it is more compatible (Ling et al., 2007). The upward change indicates less derivation of radiogenic Sr in the carbonate from the siliciclastic sediment and more influence from the water it precipitated from.

As previously mentioned, one fairly consistent signature present within the majority of the REE patterns from the middle stratigraphy of the Espanola Formation carbonates is a depletion in the light REEs relative to PAAS. Light REE depletion is a feature that has also been noted from some Neoproterozoic cap carbonates and is suggested to be characteristic of precipitation from marine waters (Zhang and Nozaki, 1996; Font et al., 2006; Huang et al., 2011; Meyer et al., 2012) and Archean hydrothermal influenced sediment when PAAS normalized (Bau and Dulski, 1996; Planavsky et al., 2010), though the depletion exhibited by the Espanola samples is less than that of modern seawater. Similarly, samples collected from another Paleoproterozoic cap carbonate, the Sausar Group in India by Mohanty et al. (2015), also had enrichment of heavy REEs relative to light REEs, which was interpreted to indicate a marine origin for the carbonates. Generally speaking, a depletion of light REEs relative to heavy REEs is a common feature of well-mixed seawater (Elderfield and Greaves, 1982; Derry and Jacobsen, 1990; Piepgras and Jacobsen, 1992; Bertram and Elderfield, 1993; Alibo and Nozaki, 1999;) and is the result of light REEs being more susceptible to absorption reactions, resulting in their preferential removal from solution (Cantrell and Byrne, 1987; Byrne and Kim, 1990; Sholkovitz et al., 1994). This further indicates a transition to greater seawater influence up-section away from the iceberg rafted debris zone. However, Y/Ho ratios of samples, primarily from the middle Espanola Formation, are predominantly less than 40, a characteristic of non-marine water, as exemplified by Figure 6 and a study by Li et al. (2019) comparing Y/Ho ratios in modern lacustrine and marine ooids. Thus, the water from which carbonate precipitated has characteristics of both seawater and non-marine water indicating a mixing of the two.

6.1.3 Upper Espanola Formation

These sediments are most common in the northernmost areas of the basin, possibly indicating deposition during maximum transgression. Here iron and manganese enriched dolostone layers with positive Eu anomalies are present interbedded with limestone and siliciclastics (Figure 3E, F). The Paleoproterozoic cap carbonate in the Sausar Group in India also has high Fe and Mn contents in the carbonate (Mohanty et al., 2015; Sarangi et al., 2017). Both an enrichment of Fe and Mn and mild to strong positive Eu anomalies are present within some Neoproterozoic cap carbonates as well (cf. Huang et al., 2011; Meyer et al., 2012; Verdel et al., 2018). The positive Eu anomalies in Espanola ferronian dolomites are similar in magnitude to those identified by Meyer et al. (2012) from the Scout Mountain Member in Idaho, which is a Sturtian cap carbonate. It has been suggested that the positive Eu anomalies observed in some of the Ediacaran cap carbonates were produced by increased weathering of detrital feldspars that would occur in the greenhouse conditions during the interglacial (Verdel et al., 2018). However, the Espanola dolostone's Fe and Mn enrichments, which occur with the positive Eu anomalies, are not explained by this process. Alternatively, positive Eu anomalies and high Fe and Mn concentrations in Neoproterozoic cap carbonates have been suggested as representative of hydrothermal input (Huang et al., 2011; Meyer et al., 2012). Young (2013a) applied this interpretation to the Espanola carbonates to conclude that they were deposited in a restricted rift basin. This view suffers from the fact that precipitates from ambient seawater from proceeding and through the time period the Espanola Formation was deposited have positive Eu anomalies (Bau and Dulski, 1996; and Danielson et al., 1992; Planavsky et al., 2010, respectively). Also, Young's (2013a) assertion is incompatible with the majority of the Espanola carbonates not having a positive Eu anomaly (Figure 4). Given that the majority of the Espanola Formation carbonates have either a mild or no positive Eu anomaly, it seems highly unlikely that

hydrothermal activity had a strong influence on the geochemical composition of most of the carbonate fraction. The precipitation of iron and manganese enriched dolostone layers in the upper Espanola Formation with positive Eu anomalies and LREE depletion can best be explained as the result of an increasing dominance of Paleoproterozoic seawater on the shallow shelf. However, this does not explain the ubiquitous MREE enrichments.

The enrichment of MREEs in the Espanola interlayered carbonate and siltstone is not compatible with patterns from modern seawater which do not display this enrichment. Hat-shaped MREE enriched patterns are believed to be derived from either preferential adsorption of light REEs on Mn-oxides and heavy REEs on Fe-oxides removing them from solution, or dissolution of phosphate minerals (Byrne et al., 1996; Rasmussen et al., 1998; Hannigan and Sholkovitz, 2001; Haley et al., 2004; Surya Prakash et al., 2012; Soyol-Erdene and Huh, 2013; Kang et al., 2014). Middle REE enrichment in some dolomite samples from the Ediacaran Doushantuo cap carbonate in China was suggested by Zhao et al. (2018) to be derived from the release of middle REE from Fe-Mn oxides during diagenesis. It is unknown what the direct cause of the middle REE enrichment is in the Espanola Formation carbonate samples, but one possible explanation is that it may be the result of varying input from riverine sources. REEs derived from riverine precipitates are noted to have highly variable patterns and can display light, middle, or heavy REE enrichments (e.g. Elderfield and Greaves, 1982; Leybourne and Johannesson, 2008). Therefore, it may be the fluctuating input of riverine water with a middle REE enrichment, coupled with marine waters with light REE depletion, a common state of both ancient and modern seawater, which influenced the REE patterns of the majority of the Espanola Formation carbonates. A recent study completed on REE distribution in the modern northeast Atlantic by

Crocket et al. (2018) found that greater interaction with continental margin sediments and terrigenous inputs led to higher light REE and middle REE concentrations in seawater. Marine sediments and pore waters on continental margins have elevated light and middle REE concentrations relative to seawater (Abbott et al., 2015) and REE patterns produced by Crocket et al. (2018, see Figure 9B) for potential REE sources to seawater from organic matter, volcanic ash, and pore waters are very similar to some patterns from carbonates of the Espanola Formation, including the middle REE enrichment and rare mild positive Eu anomalies. However, it is not necessary to attribute the positive Eu anomalies to this process as Paleoproterozoic seawater inherently has a hydrothermally-derived positive Eu anomaly (Danielson et al., 1992; Planavsky et al., 2010). Therefore the geochemistry of the upper Espanola Formation carbonates is suggested to represent a combination of influence by seawater and riverine input on a continental margin environment. The light REE depletion, heavy REE enrichment, positive Eu anomalies, and Fe and Mn enrichment are suggested to be features reflective of the seawater signature. This signature is then modified to varying degrees by riverine influx and interaction with continental shelf sediments that have enrichment in light and middle REEs. The addition of these two signatures results in a less drastic depletion in light REEs and a varying enrichment of middle REEs that can impart a 'hat-shaped' pattern.

7.1 Comparisons with Neoproterozoic Cap Carbonates

Previous discussions have highlighted the similarities between the Paleoproterozoic Espanola cap carbonate and those associated with the Neoproterozoic Sturtian and Marinoan glaciations. Here some of the differences will be discussed. Comparison of the Espanola Formation to

Neoproterozoic cap carbonates is convoluted by the fact that there are lithological and isotopic differences between even Sturtian and Marinoan cap carbonates that complicate the idea of a uniform theory to explain their mechanism of deposition (Kennedy et al., 1998; Halverson and Shields, 2011).

Bekker et al. (2005) suggested that the Espanola Formation represents a 'cap carbonate' akin in some ways to Neoproterozoic cap carbonates because of their similar tectonic settings, their largely subtidal deposition, and depletion in $\delta^{13}C$. One inconsistency that Bekker et al. (2005) outlined was a lack of stratigraphic or facies-related trends in the $\delta^{13}C$ values, whereas Neoproterozoic cap carbonates record $\delta^{13}C$ trends with time and basin position (cf. Kennedy et al., 1996; Hoffman et al., 1998; Halverson et al., 2002). However, a trend of broadly increasing $\delta^{13}C_{carb}$ values from ~-4‰ to -2.5‰ preserved within drill hole E150-2 is startlingly similar to the values previously collected from drill hole E150-1 by Bekker et al. (2005) and suggests that there is stratigraphic control on $\delta^{13}C$. This trend of upward increasing $\delta^{13}C$ in the Espanola Formation stratigraphy falls within a similar pattern to what is observed in a Neoproterozoic cap carbonate from South Australia (Giddings and Wallace, 2009) and is suggested to be the result of a broadly shallowing upwards sequence based on the observation that shallow-water carbonates are $\delta^{13}C$ enriched relative to their deep-water counterparts (cf. James et al., 2001; Hoffman et al., 2007; Jiang et al., 2007). This interpretation fits well with what is recognizable from the sedimentology of the Espanola Formation. One possible explanation for this trend is that it is a reflection of upwelling of lighter C bearing deep water having a stronger influence on the lower and middle stratigraphy, with the gradual shallowing and migration of the shoreline causing a decrease in this influence with time. This process is observed in modern systems (cf. Grotzinger

and Knoll, 1995) and has been suggested as a possible mechanism for the systematic trend of lower $\delta^{13}C$ in deeper water carbonates of the cap carbonate in the Windemere Supergroup in northwestern Canada (James et al., 2001). Lower amounts of organic matter associated with the Paleoproterozoic Espanola Formation may suggest that this process is inadequate to explain the trend in this instance. A possible alternative explanation could be that the trend is a result of a gradual decrease in the amount of influence of meltwater with time.

Another discrepancy between Neoproterozoic cap carbonates and the Espanola Formation is the lack of a basal cap dolostone unit in the Espanola Formation. These are thin basal transgressive tracts of cap carbonate sequences commonly associated with Neoproterozoic cap carbonates (Hoffman and Schrag, 2002). Within cap dolostones are a distinctive suite of sedimentary and biogenic structures such as giant wave ripples (Allen and Hoffman, 2005), sheet-crack cements, roll-up structures, and tube-like stromatolites (cf. Hoffman and Schrag, 2002; Corsetti and Kaufman, 2003). Bekker et al. (2005) suggested that some of the structures unique to the Neoproterozoic cap carbonates may be due to higher rates of inorganic precipitation as a result of supersaturation of carbonate alkalinity and that oceanic carbonate saturation may have been lower associated with the Paleoproterozoic glacial events. This explanation would fit well with the observation that several of the sedimentary structures such as sheet cracks and roll-up structures are present on Archean carbonate platforms and have been attributed to high carbonate alkalinities (Simonson et al., 1993; Sumner and Grotzinger, 2000). The unusual giant wave ripples are believed to be reflective of high storm intensity due to greater surface temperature gradients following deglaciation (Emanuel, 1987; Hoffman and Schrag, 2002). An alternative explanation for the lack of a cap dolostone unit in the Espanola Formation suggests that it can be

largely attributed to a depth and depositional environment factor. The unique sedimentary structures associated with cap dolostones, including sorted peloids, low-angle cross-bedding, stromatolites, and wave ripples indicate that cap dolostones formed above wave base (Hoffman, 2011). Given the interpretation of the lower Espanola Formation being deposited predominantly in a deeper shelf environment, it does not seem unusual that a cap dolostone is not preserved at the base of the Formation. A caviet to this is that the 1.5 m thick layer with high Ba values is close to the base of the carbonate and is dolomite, though it appears to be very laterally restricted.

One last discrepancy between Neoproterozoic cap carbonates and the Espanola Formation that was outlined by Young (2013a) is the incorporation of larger amounts of siliciclastics within the Espanola Formation, which adds considerable thickness to the stratigraphy. Young (2013a) considered this to be an important distinction between the Espanola Formation and the Neoproterozoic cap carbonates because of the interpretation that Neoproterozoic cap carbonates formed rapidly and coincidentally with post-glacial sea-level rise, prior to the introduction of siliciclastics (Hoffman et al., 1998; Hoffman, 2011). The greater incorporation of siliciclastics in the Espanola Formation, and apparent reduced carbonate precipitation, can likely be explained by the same interpretations put forth by Bekker et al. (2005) to explain the lack of specific sedimentary structures; i.e. an overall lower oceanic carbonate saturation. Analysis of the chemical index of alteration from mature siliciclastics of the Huronian Supergroup and the laterally correlative Snowy Pass Supergroup indicate extreme weathering during the Espanola-Serpent interglacial (Houston et al., 1981; Nesbitt and Young, 1982; Bekker, 1998). Relatively lower carbonate saturation conditions following the Bruce

glacial event would indicate that precipitation of the carbonate fraction in the Espanola Formation may have been more dependent upon continent-derived alkalinity than its Neoproterozoic counterparts. Furthermore, carbonate accumulation would also be dependent upon an intricate balance between the introduction of alkalinity to seawater by high weathering rates and the subsequent oceanic drop in pH and rise in carbonate compensation depth (Bekker et al., 2005).

8.1 Conclusions

The Bruce glacial event represents the second of three glacial cycles preserved in the Paleoproterozoic Huronian Supergroup, a ~12 km thick sequence of mostly sedimentary rocks that lies along the southern margin of Superior Province. The sedimentological evidence suggests that the Bruce glacial event took place on a passive, divergent margin. The overlying cap carbonates of the Espanola Formation record a gradual transition from a deeper, offshore environment, to a shallow, nearshore setting. The lower stratigraphy is dominated by deposits of rain-out such as the laminated carbonate and siltstone facies. The middle to upper stratigraphy of the Espanola Formation record a gradual shallowing upward trend with a shift to a predominance of cross-stratification, ripple lamination, hummocky cross-lamination, and intraformational conglomerate beds. These units were deposited in a nearshore environment experiencing varying influence by tide, storm, and wave activity. The geochemistry of the Espanola Formation is consistent with the sedimentological interpretation and also provides evidence that the Espanola Formation carbonates were deposited through similar processes and under similar conditions to some Neoproterozoic cap carbonates.

The stratigraphically lowest carbonate bearing unit consists of carbonate, siltstone and dropstones in the uppermost Bruce Formation. The negative $\delta^{13}C_{carb}$ excursion in this facies is on the same order of magnitude as the Wonoka-Shuram anomaly (cf. Halverson et al., 2005). It is probably the result of highly reducing fluids derived from either methane seepage promoted during deglacial warming or generation of light carbon due to oxidation of organic matter and liberation of the resulting light HCO_3^- into a stratified water column. The REE patterns for carbonate from the ice rafted debris-rich, interlayered carbonate and siltstone, which contains very light C_{carb}, are also anomalous, with negative Eu anomalies. Highly reducing conditions produced by the presence of methane or intense oxidation of organic matter are capable of reducing Eu causing an increase in solubility and therefor a reduction in its precipitation associated with the carbonate (cf. MacRae et al., 1992; Roberts et al., 2009; Sawlowitz, 2013). These sediments also have a radiogenic $^{87}Sr/^{86}Sr$ ratio, which indicates mobilization of ^{87}Sr, produced by radioactive decay, into the carbonate phases. εNd(0) in carbonates in the uppermost Bruce Formation associated with glacial rainout is similar to values from Holocene carbonates associated with glacial rainout in the northeastern Atlantic (cf. Blaser et al, 2019). In both cases the source on the sediment was Superior Province and the anomalous εNd(0) values are due to diagenetic interaction between the siliciclastics and carbonate. All of this data are compatible with the carbonate-siltstone-dropstone unit in the uppermost Bruce Formation being deposited under a layer of stratified bottom water. Highly reducing conditions were created either by methane release into, and from, the sediment or significant oxidation of organic matter. These conditions resulted in diagenetic geochemical interaction between the siliciclastic and carbonate phases producing distinctive chemical traits in the carbonate.

At the base of the Espanola, above the dropstone-bearing unit, there is an increase in $\delta^{13}C$ from -4.5‰ to -2‰, which may represent disintegration of the stratified water mass, which produced the underlying carbonates with $\delta^{13}C$ of -10‰, and incursion of well-mixed seawater. A thin dolomite succession highly enriched in Ba is also present in this interval and likewise indicates marine incursion. The interval is ended by a return to -4‰ followed by a very gradual increase in $\delta^{13}C$ over 110 m to -2.5‰. This is similar to trends that have been observed in a Cryogenian cap carbonate in South Australia and there was interpreted to be the result of an upwards shallowing (Giddings and Wallace, 2009). This is consistent with sedimentological evidence. However, shallowing would also entail closer proximity to the shoreline and freshwater runoff, which would lower the $\delta^{13}C$ value. The preferred model is a freshwater dominated surface layer, which facilitated the reduction in $\delta^{13}C$ to -4‰, gradually dissipated and became more seawater dominant through time.

The REE patterns are consistent through this thick section of the Espanola. They are LREE depleted, similar to seawater, but also are variably MREE enriched. Freshwater, rather than seawater is a reasonable source for the enrichment. The $^{87}Sr/^{86}Sr$ ratio is less radiogenic throughout this succession than the underlying carbonate-siltstone-dropstone unit, denoting a decrease in interaction between the siliciclastic and carbonate phases. The $\varepsilon Nd(2400)$ for carbonate in this thick middle section of the Espanola Formation is similar to carbonate deposited in the Holocene of the northeastern Atlantic during deglaciation (cf. Blaser et al., 2019), indicating seawater derivation for this LREE.

The trend to increased seawater dominance over freshwater continues into the upper Espanola Formation, as evidenced by sediment deposited during maximum flooding of the northern-most portion of the basin. Dolomite layers enriched in iron and manganese appear for the first time. The REE patterns for these layers, and even some associated limestone layers, are distinctive with positive Eu anomalies. These geochemical traits are characteristic of ocean chemistry in the Paleoproterozoic (Danielson et al., 1992; Planavsky et al., 2010).

The uppermost Espanola Formation sediments gradually transition into sandstones of the lower Serpent Formation via an overall decrease, and subsequent loss, of carbonate-rich interbeds. Carbonate-rich interbeds occur in packages alongside sandstones with trough cross-stratification, ripple lamination, parallel lamination, and hummocky cross-stratification. Deposition of the lower Serpent Formation was in a nearshore to fluvial environment with evidence of tidal influence.

The new geochemical and isotopic evidence presented in this study highlights that there are more similarities between the Espanola Formation and Neoproterozoic cap carbonates than previously known. Some parallels also exist between the Espanola Formation and the Sausar Group in India; another probable Paleoproterozoic cap carbonate (Mohanty et al., 2014; Sarangi et al., 2017). The considerable geochemical similarities between Neoproterozoic and Paleoproterozoic cap carbonates indicate that the evolution of water mass geochemistry in both time periods probably had a large amount of commonality. This strongly indicates that the Paleoproterozoic middle Huronian glaciation was extreme, probably resulting in the development of snowball or slushball conditions.

Acknowledgements

This work was supported by a Natural Science and Engineering Research Council of Canada Graduate Scholarship to SK and a Natural Science and Engineering Research Council of Canada Discovery Grant to PF, as well as European Union's Horizon 2020 Research and Innovation Programme Council (grant agreement no 716515 to SL). We thank two anonymous reviewers for very helpful comments. Drafting was performed by Jordan Heroux.

References

Abbott, A.N., Haley, B.A., McManus, J. and Reimers, C.E., 2015. The sedimentary flux of dissolved rare earth elements to the ocean. Geochimica et Cosmochimica Acta, 154, 186-200.

Aigner, T. and Reineck, H.-E., 1982. Proximality trends in modern storm sands from the Helegoland Bight (North Sea) and their implications for basin analysis. Senckenbergiana Maritime 14, 183-215.

Alibo, D. S. and Nozaki, Y., 1999. Rare earth elements in seawater: particle association, shale normalization, and Ce oxidation. Geochimica et Cosmochimica Acta 63, 363–372.

Allen, P.A. and Hoffman, P.F., 2005. Extreme winds and waves in the aftermath of a Neoproterozoic glaciation. Nature 433, 123-127.

Aloisi, G., Bouloubassi, I., Heijs, S.K., Pancost, R.D., Pierre, C., Damste, J.S.S., Gottschal, J.C., Forney, L.J. and Rouchy, J.M., 2002. CH_4-consuming microorganisms and the formation of carbonate crusts at cold seeps. Earth and Planetary Science Letters 203, 195–203.

Angelier, J., 1985. Extension and rifting: the Zeit region, Gulf of Suez. Journal of Structural Geology 7, 605-612,

Arne, M. and Montenari, M., 2008. A snowball Earth versus a slushball Earth: Results from Neoproterozoic climate modelling sensitivity experiments. Geosphere 4, 401-410.

Axen, G.J., Grove, M., Stockli, D., Lovera, O.M., Rothstein, D.A., Fletcher, J.M., Farley, K. and Abbott, P.L., 2000. Thermal evolution of Monte Blanco Dome; low-angle normal faulting during Gulf of California rifting and late Eocene denudation of the eastern Peninsular Ranges. Tectonics 2, 197-212.

Bates, M.P, and Halls, H.C., 1990. Regional variation in paleomagnetic polarity of the Matachewan dyke swarm related to the Kapuskasing Structural Zone, Ontario. Canadian Journal of Earth Science 27, 200-211.

Bau, M. and Dulski, P., 1996. Distribution of yttrium and rare-earth elements in the Penge and

Kuruman iron-formations, Transvaal Supergroup, South Africa. Precambrian Research 79, 37–55.

Bau, M., Dulski, P. and Möller, P., 1995. Yttrium and holmium is South Pacific seawater: vertical distribution and possible fractionation mechanisms. Chem Erde 55, 1-15.

Bayet-Goll, A., De Carvalho, C.N., Moussavi-Harami, R., Mahboubi and A., Nasiri, Y., 2014. Depositional environments and ichnology of the deep-marine succession of the Amiran Formation (upper Maastrichtian-Paleocene), Lurestan Province, Zagros Fold- Thrust Belt, Iran. Palaeogeography Palaeoclimatology Palaeoecology 401, 13–42.

Bayon, G., Dupré, S., Ponzevera, E., Etoubleau, J., Chéron, S., Pierre, C., Mascle, J., Boetius, A. and de Lange, G., 2013. Formation of carbonate chimneys in the Mediterranean Sea linked to deep-water oxygen depletion. Nature Geoscience 6, 755–760.

Beh, B., 2012. Depositional processes operating on the Paleoproterozoic ice margin. MSc Thesis, Lakehead University, Thunder Bay, Ontario, Canada, 195p.

Baker, P.A., Kastner, M. and Anderson, G.E., 1981.Mechanism and kinetics of sulfate inhibition on dolomitization of calcium carbonate. American Association of Petroleum Geologists Bulletin 65, 893.

Bekker, A., 1998. Chemostratigraphy and climatostratigraphy of the Paleoproterozoic Snowy

Pass Supergroup, Wyoming and its application for correlation with other sequences in North America. M.Sc. thesis, University of Minnesota, Duluth, 104p.

Bekker, A., and Karhu, J. A., 1996. Study of carbon isotope ratios in carbonates of the Early Proterozoic Snowy Pass Supergroup, WY and its application for correlation with the Chocolay Group, MI and Huronian Supergroup, ON [abstract]: Institute on Lake Superior Geology, 42nd Annual Meeting, Cable, Wisconsin, 1996, Proceedings 42 (1), 4–5.

Bekker, A., Eriksson, K. A., Kaufman, A. J., Karhu, J. A., and Beukes, N. J., 1999. Paleoproterozoic record of biogeochemical events and ice ages: Geological Society of America, Annual Meeting, Abstracts with Programs 31 (7), A-487.

Bekker, A., Kaufman, A.J., Karhu, J.A., Beukes, N.J., Swart, Q.D., Coetzee, L.L. and Eriksson, K.A., 2001. Chemostratigraphy of the Paleoproterozoic Duitschland Formation, South Africa: implications for coupled climate change and carbon cycling. American Journal of Science 301, 261–285.

Bekker, A., Sial, A.N., Karhu, J.A., Ferrerira, V.P., Noce, G.M., Kaufman, A.J., Romano, A.W. and Pimental, M.M., 2003. Chemostratigraphy of carbonates from the Minas Supergroup, Quadrilatero Ferrifero (Iron Quadrangle), Brazil: a stratigraphic record of Early Proterozoic atmospheric, biogeochemical, and climatic change. American Journal of Science 303, 865-904.

Bekker, A., Holland, H.D., Wang, P.-L., Rumble, D., Stein, H.J., Hannah, J.L., Coetzee, L.L. and Beukes, N.J., 2004. Dating the rise of atmospheric oxygen. Nature, 427, 117-120.

Bekker, A., Kaufman, A.J., Karhu, J.A. and Eriksson, K.A., 2005. Evidence for Paleoproterozoic cap carbonates in North America. Precambrian Research 137, 167–206.

Bennett, G., 2006. The Huronian Supergroup between Sault Ste Marie and Elliot Lake. Field Trip Guidebook. Institute on Lake Superior Geology 52, 1–65.

Bennett, G., Dressler, B.O. and Robertson, J.A., 1991. The Huronian Supergroup. In: Geology of Ontario. Ontario Geological Survey, pp. 549–591, Special Volume 4, Part 1.

Bernstein, L. and Young, G.M., 1990. Depositional environments of the Early Proterozoic Espanola Formation, Ontario, Canada. Canadian Journal of Earth Science 27, 539–551.

Bertram, C. J.and Elderfield, H., 1993. The geochemical balance of the rare-earth elements and neodymium isotopes in the oceans. Geochimica et Cosmochimica Acta 57, 1957–1986.

Blaser, P., Poppelmeier, F., Schulz, H., Gutjahr, M., Frank, M., Lippold, J., Heinrich, H., Link, J.M., Hoffmann, J., Szidat, S. and Frank, N., 2019. The resilience and sensitivity of Northeast Atlantic deep water εNd to overprinting by detrital fluxes over the past 30,000 years. Geochimica et Cosmochimica Acta 245, 79-97.

Bolhar, R. and Van Kranendonk, M.J., 2007. A non-marine depositional setting for the northern Fortescue Group, Pilbara craton, inferred from trace element geochemistry of stromatolitic carbonates. Precambrian Research 155, 229-250.

Bolhar, R., Kamber, B.S., Moorebath, S., Fedo, C.M. and Whitehouse, M.J., 2004. Characterization of early Archean chemical sediments by trace element signatures. Earth and Planetary Science Letters 222, 43-60.

Bond, G.C., Kominz, M.A. and Sheridan, R.E., 1995. Continental terraces and rises. In, ed. by C.J. Busby and R.V. Ingersoll, Tectonics of Sedimentary Basins. Blackwell Science, Cambridge Mass., 119-148.d

Bourgeois, J. and Leithold, E.L., 1984. Wave reworked conglomerates – depositional processes and criteria for recognition. In, ed. By E.H. Koster snd R.J. Steel, Sedimentology of Gravels and Conglomerates. Memoir Canadian Society of Petroleum Geologists, 10, 331-343.

Byrne, R. H., Kim and K. H., 1990. Rare-earth element scavenging in seawater. Geochimica et Cosmochimica Acta 54, 2645–2656.

Byrne, R.H., Xuewu, L. and Schuf, J., 1996. The influence of phosphate coprecipitation on rare earth element distributions in natural waters. Geochimica et Cosmochimica Acta 60, 3341-3346.

Campbell, T.J., Richards, F.W., Silva, R.L., Wach, G. and Eliuk, L., 2015. Interpretation of the Penobscot 3D seismic volume using constrained sparse spike inversion, Sable sub-Basin, offshore Nova Scotia. Marine and Petroleum Geology 68, 73-93.

Cantrell, K. J. and Byrne, R. H., 1987. Rare-earth element complexation by carbonate and oxalate ions. Geochimica et Cosmochimica Acta 51, 597-605.

Card, K.D., Innes, D.G. and Debicki, R.L., 1977. Stratigraphy, sedimentology, and petrology of the Huronian Supergroup in the Sudbury-Espanola area. Ontario Division of Mines, Geoscience Study 16, 99p.

Caxito, F.A., Frei, R., Uhlein, G.J., Dias, T.G., Arting, T.B. and Uhlein, A., 2018. Multiproxy geochemical and isotopic stratigraphy records of a Neoproterozoic oxygenation event in the Ediacaran Sete Lagoas cap carbonate, Bambui Group, Brazil. Chemical Geology 481, 119-132.

Chen, Y.J., Chen, W.Y., Li, Q.G., Santosh,M. and Li, J.R., 2019. Discovery of the Huronian glaciation event in China: evidence from glacigenic diamictites in the Hutuo Group in Wutai Shan. Precambrian Research, 320, 1-12.

Chorowicz, J., 2005. The East African Rift system. Journal of African Earth Sciences 43, 379-410.

Closs, H., 1939. Hebung-Spaltung-Vulkanismus. Geologische Rundschau 30, 405-525.

Collins, W.H., 1925. North Shore of Lake Huron. Geological Survey of Canada Memoir 143.

Corsetti, F.A. and Kaufman, A.J., 2003. Stratigraphic investigations of carbon isotope anomalies and Neoproterozoic ice ages in Death valley, California. Geological Society of America Bulletin 115, 916–932.

Corsetti, F.A. and Lorentz, N.J., 2006. On Neoproterozoic cap carbonates as chronostratigraphic markers. In: Xiao, S., and Kaufman, A.J. (Eds.), Neoproterozoic geobiology and paleobiology. Dordrecht, Springer, 273–294.

Cox, K.G., 1989. The role of mantle plumes in the development of continental drainage patterns. Nature 342, 873-877.

Crocket, K.C., Hill, E., Abell, R.E., Johnson, C., Gary, S.F., Brand, T. and Hathorne, E.C., 2018. Rare earth element distribution in the NE Atlantic: evidence for benthic sources, longevity of the seawater signal, and biogeochemical cycling. Frontiers in Marine Science 5 (147), 1-22.

Danielson, A., Moller, P. and Dulski, P., 1992. The europium anomalies in banded iron formations and the thermal history of the ocean crust. Chemical Geology 97, 89-100.

Davis, P.M. and Slack, P.D., 2002. The uppermost mantle beneath the Kenya dome and relation to melting, rifting and uplift in East Africa. Geophysical Research Letters 29, 21-1 – 21-4.

de Alvarenga, C.J.S., Santos, R. V. and Dantas, E.L., 2004. C-O-Sr isotopic stratigraphy of cap carbonates overlying Marinoan-age glacial diamictites in the Paraguay Belt, Brazil. Precambrian Research 131, 1–21.

Demicco, R.V., 1983. Wavy and lenticular-bedded carbonate ribbon rocks of the Upper Cambrian Conococheague Limestone, Central Appalachians. Journal of Sedimentary Petrology 53, 1121–1132.

Denyszyn, S.W., Davis, D.W. and Halls, H.C., 2009. Paleomagnetism and U-Pb geochronology of the Clarence Head dykes, Arctic Canada: orthogonal emplacement of mafic dykes in a large igneous province. Canadian Journal of Earth Sciences 46, 155-167.

Derry, L.A. and Jacobsen, S.B., 1990. The chemical evolution of Precambrian seawater – evidence from REEs in banded iron formations. Geochimica et Cosmochimica Acta 54 (11), 2965–2977.

Dickinson, W.R., 1985. Interpreting provenance relations from detrital modes of sandstone. In, ed. G.G. Zuffa, Provenance of Arenites, D. Reidel, Dordrecht, 333-361.

Dietrich, P., Ghienne, J.-F., Schuster, M., LaJeunesse, P., Nutz, A., Deschamps, R., Roquin, C. and Duringer, P., 2017. From outwash to costal systems in the Portneuf-Forestville deltaic

complex (Quebec North Shore): Anatomy of a forced regressive deglacial sequence. Sedimentology 64, 1044-1078.

Eggertson, E B., 1975. The Espanola Formation; a Proterozoic carbonate north of Lake Huron, Ontario. Bachelor's Thesis, McMaster University, Hamilton, Ontario, 97p.

Elderfield, H. and Greaves, M. J., 1982. The rare-earth elements in sea-water. Nature 296, 214–219.

Emanuel, K.A., 1987. The dependence of hurricane intensity on climate. Nature 326, 483–485.

Evans, D.A., Beukes, N.J. and Kirschvink, J.L., 1997. Low-latitude glaciation in the Paleoproterozoic era. Nature 386, 262-266.

Eyles, N. and Januszczak, N., 2004. 'Zipper-rift': a tectonic model for Neoproterozoic glaciations during the breakup of Rodinia after 750 Ma. Earth Science Reviews 65, 1-73.

Farquhar, J., Bao, H. and Thiemens, M, 2000. Atmospheric influence of Earth's earliest sulfur cycle. Science 289, 756-758.

Favre, P. and Stampfli, G.M., 1992. From rifting to passive margin; the examples of the Red Sea, central Atlantic and Alpine Tethys. Tectonophysics 215, 69-97.

Font, E., Nédélec, A., Trindade, R.I.F., Macouin, M. and Charrière, A. 2006. Chemostratigraphy of the Neoproterozoic Mirassol d'Oeste cap dolostones (Mato Grosso, Brazil): an alternative model for Marinoan cap dolostone formation. Earth and Planetary Science Letters 250, 89–103.

Fralick, P.W., 1984. Deposition on an Early Proterozoic continental margin: the lower Huronian Supergroup of central Ontario. Geological Association of Canada, Abstract, 9, p. 63.

Fralick, P.W., 1985. Early Proterozoic basin development on a cratonic margin: the lower Huronian Supergroup of central Ontario. Ph.D. Thesis, University of Toronto, Toronto, Ontario, 466p.

Fralick, P.W. and Miall, A.D., 1981. Sedimentology of the Matinenda Formation. Ontario Geologic Survey, Miscellaneous Paper 98, 80-89.

Fralick, P.W. and Miall, A.D.,1987. Glacial outwash uranium placers? Evidence from the lower Huronian Supergroup, Ontario, Canada. In: (ed. D. Pretorius) Uranium Deposits in Proterozoic Quartz-Pebble Conglomerates. International Atomic Energy Agency, Vienna, IAEA-TECDOC 427, 133-154.

Fralick, P.W. and Miall, A.D., 1989. Sedimentology of the Lower Huronian Supergroup (Early Proterozoic), Elliot Lake area, Ontario, Canada. Sedimentary Geology 63, 127–153.

Fralick, P.W. and Riding, R., 2015. Steep Rock Lake: Sedimentology and geochemistry of an Archean carbonate platform. Earth-Science Reviews 151, 132-175.

Frarey, M.J. and Roscoe, S.M., 1971. The Huronian Supergroup north of Lake Huron. In: Symposium on Basins and Geosynclines of the Canadian Shield. Geological Survey of Canada, Paper 70-40, 143–158.

Giddings, J.A. and Wallace, M.W., 2009. Sedimentology and C-isotope geochemistry of the "Sturtian" cap carbonate, South Australia. Sedimentary Geology 216, 1–14.

Grasse, P., Bosse, L., Hathorne, E.C., Boning, P., Pahnke, K. and Frank, M., 2017. Short-term variability of dissolved rare earth elements and neodymium isotopes in the entire water column of the Panama Basin. Geochimica et Cosmochimica Acta 475, 242-253.

Grotzinger, J.P., 1986. Evolution of Early Proterozoic passive- margin carbonate platform, Rocknest Formation, Wopmay Orogen, Northwest Territories. Journal of Sedimentary Petrology, 56, 831– 847.

Grotzinger, J.P. and Knoll, A. H., 1995. Anomalous carbonate precipitates: is the Precambrian the key to the Permian? Palaios 10: 578–596.

Grotzinger, J.P., Fike, D.A. and Fischer, W.W., 2011. Enigmatic origin of the largest-known carbon isotope excursion in Earth's history. Nature Geoscience 4, 285-292.

Gumsley, A.P., Chamberlain, K.R., Bleeker, W., Soderlund, U., de Kock, M.O., Larsson, E.R and Bekker, A., 2017. Timing and tempo of the Great Oxidation Event. PNAS 114, 1811-1816.

Haley, B.A., Klinkhammer, G.P. and McManus, J., 2004. Rare earth elements in pore waters of marine sediments. Geochimica et Cosmochimica Acta 68, 1265-1279.

Halverson, G.P., Hoffman, P.F., Schrag, D.P. and Kaufman, A.J., 2002. A major perturbation of the carbon cycle before the Ghaub glaciation (Neoproterozoic) in Namibia: Prelude to snowball Earth? Geochemistry, Geophysics, Geosystems 3 (6), 16p.

Halverson, G.P., Hoffman, P.F., Schrag, D.P., Maloof, A.C. and Rice, A.H., 2005. Towards Neoproterozoic composite carbon-isotope record. Geological Society of America Bulletin 117, 1181–1207.

Halverson, G.P., Wade, B.P., Hurtgen, M.T. and Barovich, K.M., 2010. Neoproterozoic chemostratigraphy. Precambrian Research 182, 337–350.

Halverson, G. P. and Shields, G., 2011. Chemostratigraphy and the Neoproterozoic glaciations. In: Arnaud, E., Halverson, G. P., Shields, G. (Eds.), The Geological Record of Neoproterozoic Glaciations. Geological Society, London, Memoirs 36, 51–66.

Hambrey, M.J. and Harland, W.B., 1981. Earth's Pre-Pleistocene Glacial Record. Cambridge University Press, Cambridge.

Hannigan, R.E. and Sholkovitz, E.R., 2001. The development of middle rare earth element enrichment in freshwaters; weathering of phosphate minerals. Chemical Geology 175, 495-508.

Hilburn, I.A., Joseph, L., Kirschvink, J.L., Tajikab, E., Tadab, R., Hamanob, Y. and Yamamotob, S., 2005. A negative fold test on the Lorrain Formation of the Huronian Supergroup: uncertainty on the paleolatitude of the Paleoproterozoic Gowganda glaciation and implications for the great oxygenation event. Earth and Planetary Science Letters 232, 315–332.

Hoffman, P.F., 2011. Strange bedfellows: glacial diamictite and cap carbonate from the Marinoan (635 Ma) glaciations in Namibia. Sedimentology 58, 57-119.

Hoffman, P.F., 2013. The Great Oxidation and a Siderian snowball Earth: MIF-S based correlation of Paleoproterozoic glacial epochs. Chemical Geology 362, 143-156.

Hoffman, P.F. and Schrag, D.P., 2002. The snowball earth hypothesis: testing the limits of global change. Terra Nova 14, 129–155.

Hoffman, P.F., Kaufman, A.J., Halverson, G.P. and Schrag, D.P., 1998. A Neoproterozoic snowball Earth. Science, 281, 1342-1346.

Hoffman, P. F., Halverson, G. P., Domack, E. W., Husson, J. M., Higgins, J. A. and Schrag, D. P., 2007. Are basal Ediacaran (635Ma) post-glacial 'cap dolostones' diachronous?. Earth and Planetary Science Letters 258, 114–131.

Hoffmann, K.H., Condon, D.J., Bowring, S.A. and Crowley, J.L., 2004. U-Pb zircon date from the Neoproterozoic Ghaub Formation, Namibia: Constraints on Marinoan glaciation. Geology 32, 817-820.

Hofmann, H.J., Pearson, D.A.B. and Wilson, B.H., 1980. Stromatolites and fenestral fabric in the early Proterozoic Huronian Supergroup, Ontario. Canadian Journal of Earth Sciences 17, 1351-1357.

Houston, R.S., Lanthier, L.R., Karlstrom, K.E. and Sylvester, G., 1981. Paleoproterozoic diamictite of southern Wyoming. In: Hambrey, M.J., Harland, W.B. (Eds.), Earth's Pre-Pleistocene Glacial Record. Cambridge University Press, New York, 795–799.

Hu, R., Wang, W., Li, S.-Q., Yang, Y.-Z. and Chen, F., 2016. Sedimentary environment of Ediacaran sequences of South China: trace element and Sr-Nd isotope constraints. The Journal of Geology 124, 769-789.

Huang, J., Chu, X., Jiang, G., Feng, L. and Chang, H. 2011. Hydrothermal origin of elevated iron, manganese and redox-sensitive trace elements in the ca. 635Ma Doushantuo cap carbonate. Journal of the Geological Society of London 168, 805–815.

Hutchinson, D.R., Grow, J.A., Klitgord, K.D. and Swift, B.A., 1980. Deep[structure and evolution of the Carolina trough. American Association of Petroleum Geologists Memoir 34, 129-152.

Hyde, W., Crowley, T., Baum, S. and Peltier, W., 2000. Neoproterozoic “snowball Earth” simulations with a coupled climate/ice sheet model. Nature 405, 425-429.

James, N.P., Narbonne, G.M. and Kyser T.K., 2001. Late Neoproterozoic cap carbonates: Mackenzie Mountains, northwestern Canada: precipitation and global glacial meltdown. Canadian Journal of Earth Sciences 38, 1229–1262.

Jiang, G., Kennedy, M.J. and Christie-Blick, N., 2003. Stable isotopic evidence for methane seeps in Neoproterozoic postglacial cap carbonates. Nature 426, 822–826.

Jiang, G., Kennedy, M.J., Christie-Blick, N., Wu, H. and Zhang, S., 2006a. Stratigraphy, sedimentary structures, and textures of the Late Neoproterozoic Doushantuo cap carbonate in South China. Journal of Sedimentary Research 76, 978–995.

Jiang, G., Shi, X. and Zhang, S., 2006b. Methane seeps, methane hydrate destabilization, and the late Neoproterozoic postglacial cap carbonates. Chinese Science Bulletin 51, 1152–1173.

Jiang, G., Kaufman, A.J., Christie-Blick, N., Zhang, S. and Wu, H., 2007. Carbon isotope variability across the Ediacaran Yangtze platform in South China: implications for a large surface to deep ocean δ13C gradient. Earth and Planetary Science Letters 261, 303–320.

Junnila, R.M. and Young, G.M., 1995. The Paleoproterozoic upper Gowganda Formation, Whitefish Falls area, Ontario, Canada: subaqueous deposits of a braid delta. Canadian Journal of Earth Sciences 32, 197-209.

Kang, J., Jeong, K.-S., Cho, J.H., Lee, J.H., Jang, S. and Kim, S.R., 2014. Post-depositional redistribution processes and their effects on middle rare earth element precipitation and the cerium anomaly in sediments in the South Korea Plateau, east sea. Journal of Aisian Earth Sciences 82, 66-79.

Kasemann, S.A., Prave, A.R., Fallick, A.E., Hawkesworth, C.J. and Hoffmann, K.H., 2010. Neoproterozoic ice ages, boron isotopes, and ocean acidification: Implications for a snowball Earth. Geology 38, 775–778.

Kaufman, A.J., Johnston, D.T., Farquhar, J., Masterson, A.L., Lyons, T.W., Bates, S., Anbar, A.D., Arnold, G.L., Garvin, J. and Buick, R., 2007. Late Archean biospheric oxygenation and atmospheric evolution. Science 317, 1900–1903.

Kautenberger, R., Hein, C., Sander, J.M. and Beck, H.P., 2014. Influence of metal loading and humic acid functional groups on the complexation behavior of trivalent lanthanides analysed by CE-ICP-MS. Analytica Chimica Acta 816, 50-59.

Kawabe, I., Kitahara, Y. and Naito, K., 1991. Non-chondritic yttrium/holmium ratio and lanthanide tetrad effect observed in pre-Cenozoic limestones. Geochemical Journal 25, 31-44.

Kazmierczak, J. and Goldring, R., 1978. Subtidal flat-pebble conglomerate from the Upper Devonian of Poland: a multiprovenant high-energy product. Geological Magazine 115, 359–366.

Kennedy, M.J., 1996. Stratigraphy, sedimentology and isotopic geochemistry of Australian Neoproterozoic postglacial cap dolostones: deglaciation, $\delta_{13}C$ excursions and carbonate precipitation. Journal of Sedimentary Research 66, 1050–1064.

Kennedy, M.J., Runnegar, B., Prave, A.R., Hoffmann, K.H. and Arthur, M.A., 1998. Two or four Neoproterozoic glaciations? Geology 26, 1059–1063.

Kennedy, M.J., Christie-Blick, N. and Sohl, L.E., 2001. Are Proterozoic cap carbonates and isotopic excursions a record of gas hydrate destabilization following Earth's coldest intervals? Geology 29, 443–446.

Kent, R., 1991. Lithospheric uplift in eastern Gondwana: Evidence for a long-lived mantle plume system? Geology 19, 19-23.

Ketchum, K.Y., Heaman, L.M., Bennett, G. and Hughes, D.J., 2013. Age, petrogenesis and tectonic setting of the Thessalon volcanic rocks, Huronian Supergroup, Canada. Precambrian Research 233, 144-172.

Kirschvink, J.L., 1992. Late Proterozoic low-latitude global glaciation–The Snowball Earth. In: Schopf, J.W., Klein, C. (Eds.), The Proterozoic Biosphere. Cambridge University Press, Cambridge, 51–52.

Kirschvink, J.L., Gaidos, E.J., Bertani, L.E., Beukes, N.J., Gutzmer, J., Maepa, L.N. and Steinberger, R.E., 2000. Paleoproterozoic snowball Earth: extreme climatic and geochemical global change and its biological consequences. Proceedings of the National Academy of Sciences 97, 1400-1405.

Komer, P.D., 1976. Beach Processes and Sedimentation. Prentice Hall. Englewood Cliffs, N.J., 429pp.

Kopp, R.E., Kirschvink, J.L., Hilburn, I.A. and Nash, C.Z., 2005. The Paleoproterozoic snowball Earth: A climate disaster triggered by the evolution of oxygenic photosynthesis. PNAS 102 (32), 11131-11136.

Krogh, T.E., Davis, D.W. and Corfu, F., 1984. Precise U–Pb zircon and baddeleyite ages from the Sudbury area. In: Pye, E.G., Naldrett, A.J., Giblin, P.E. (Eds.), The Geology and Ore Deposits of the Sudbury Structure. Ontario Geological Survey, Toronto, Ontario, 431–446.

Labails, C., Olivet, J.-L., Aslanian, D. and Roest, W.R., 2010. An alternative early opening scenario for the Central Atlantic Ocean. Earth and Planetary Science Letters 297, 355-368.

Leckie, D.A. and Walker, R.G., 1982. Storm- and tide-dominated shorelines in Cretaceous Moosebar-Lower Gates interval-outcrop equivalents of deep basin gas trap in western Canada. Bulletin of the American Association of Petroleum Geologists, 66, 138-157.

Lee, Y.I. and Kim, J.C., 1992. Storm-influenced siliciclastic and carbonate ramp deposits, the Lower Ordovician Dumugol Formation, South Korea. Sedimentology 39, 951– 969.

Leeder, M.R. and Gawthorpe, R.L., 1987. Sedimentary models for extensional tilt-block/half-graben basins. Geological Society of London Special Publication 28, 139-152.

Lemaitre, N., Bayon, G., Ondréas, H., Caprais, J.C., Freslon, N., Bollinger, C., Rouget, M.L., de Prunelé, A., Ruffine, L., Olu-Le Roy, K. and Sarthou, G., 2014. Trace element behaviour at cold seeps and the potential export of dissolved iron to the ocean. Earth and Planetary Science Letters 404, 376–388.

Leybourne, M.I. and Johannesson, K.H., 2008. Rare earth elements (REE) and yttrium in stream waters. Stream sediments, and Fe-Mn oxyhydroxides; fractionation, speciation, and controls over REE+Y patterns in the surface environment. Geochimica et Cosmochimica Acta 72, 5962-5983.

Li, F., Webb, G.E., Algeo, T.J., Kershaw, S., Lu, C., Oehlert, A.M., Gong, Q., Pourmand, A. and Tan, X., 2019. Modern carbonate ooids preserve ambient aqueous REE signatures. Chemical Geology 509, 163-177.

Ling, H.-F., Feng, H.-Z., Pan, J.-Y., Jiang, S.-Y., Chen, Y.-Q. and Chen, X., 2007. Carbon isotope variation through the Neoproterozoic Doushantuo and Dengying Formations, South

China: Implications for chemostratigraphy and paleoenvironmental change. Palaeogeography, Palaeoclimatology, Palaeoecology 254, 158-174.

Liu, C., Wang, Z., Raub, T.D., Macdonald, F.A. and Evans, D.A.D., 2014. Neoproterozoic cap dolostone deposition in stratified glacial meltwater plume. Earth and Planetary Science Letters 404, 22-32.

Liu, C., Wang, Z. and MacDonald, F.A., 2018. Sr and Mg isotope geochemistry of the basal Ediacaran cap limestone sequence of Mongolia: Implications for carbonate diagenesis, mixing of glacial meltwaters, and seawater chemistry in the aftermath of snowball Earth. Chemical Geology, 491, 1-13.

Long, D.G.F., 1978. Depositional environments of a thick Proterozoic sandstone: the (Huronian) Mississagi Formation of Ontario, Canada. Canadian Journal of Earth Science 15, 190-206.

Long, D.G.F., 2009. The Huronian Supergroup. In: Rousell, D.H., Brown, G.H. (Eds.), A field guide to the Geology of Sudbury, Ontario. Ontario Geological Survey, Open File Report 6243, 14-30.

Macdonald, F.A., Schmitz, M.D., Crowley, J.L., Roots, C.F., Jones, D.F., Maloof, A.C., Strauss, J.V., Cohen, P.A., Johnston, D.T. and Schrag, D.P., 2010. Calibrating the Cryoganian. Science 327, 1241-1243.

MacRae, N.D., Nesbitt, H.W. and Kronberg, B.I., 1992. Development of a positive Eu anomaly during diagenesis. Earth and Planetary Science Letters 109, 585-591.

Markello, J.R. and Read, J.F., 1982. Upper Cambrian intra- shelf basin, Nolichucky Formation, southwest Virginia Appalachians. American Association of Petroleum Geologists Bulletin 66, 860–878.

Marmo, J.S. and Ojakangas, R.W., 1984. Lower Proterozoic glaciogenic deposits, eastern Finland. Geologic Society of America Bulletin 95, 1055-1062.

Martin, D.M., 1999. Depositional setting and implications of Paleoproterozoic glaciomarine sedimentation in the Hamersley province, western Australia. Geological Society of America Bulletin 111, 189-203.

McLennan, S.M., 1989. Rare earth elements in sedimentary rocks: influence of provenance and sedimentary processes. In: Lipin, B.R., McKay, G.A. (Eds.), Geochemistry and mineralogy of rare earth elements. Mineralogical Society of America Reviews in Mineralogy 21, 169–200.

McLennan, S.M., Fryer, B.J. and Young, G.M., 1979. The geochemistry of the carbonate- rich Espanola Formation (Huronian) with emphasis on the rare earth elements. Canadian Journal of Earth Sciences 16, 230-239.

McLennan, S.M., Nance, W.B. and Taylor, S.R., 1980. Rare earth element-thorium correlations in sedimentary rocks, and the composition of the continental crust. Geochimica et Cosmochimica Acta 44, 1833–1839.

McLennan, S.M., Taylor, S.R. and Eriksson, K.A., 1983. Geochemistry of Archean shales from the Pilbara Supergroup, Western Australia. Geochimica et Cosmochimica Acta 47, 1211–1222.

McLennan, S.M., Bock, B., Hemming, S.R., Hurowitz, J.A., Lev, S.M. and McDaniel, D.K., 2003. The roles of provenance and sedimentary processes in the geochemistry of sedimentary 250 rocks. In: Lentz, D.R. (Ed.), Geochemistry of Sediments and Sedimentary Rocks: Evolutionary Considerations to Mineral Deposit-forming Environments. Geological Association of Canada, GeoText 4, 7–38.

Medina, F., 1995. Syn- and post-rift evolution of the El Jadida-Agadir basin (Morocco): constraints for the rifting models of the central Atlantic. Canadian Journal of Earth Science 32, 1273-1291.

Meyer, E.E., Quicksall, A.N., Landis, J.D., Link, P.K. and Bostick, B.C. 2012. Trace and rare earth elemental investigation of a Sturtian cap carbonate, Pocatello, Idaho: evidence for ocean redox conditions before and during carbonate deposition. Precambrian Research 192–195, 89–106.

Meyn, H.D., 1970. Geology of Hutton and Parkin Townships. Ontario Department of Mines Geology Report 80, 78p.

Miall, A.D., 1983. Glaciomarine sedimentation in the Gowganda Formation (Huronian), northern Ontario. Journal of Sedimentary Petrology 53, 477-492.

Miall, A. D., 1985. Sedimentation on an early Proterozoic continental margin; the Gowganda Formation (Huronian), Elliot Lake area, Ontario, Canada. Sedimentology 2, 763-788.

Mohanty, S.P., Barik, A., Sarangi, S. and Sarkar, A., 2015. Carbon and oxygen isotope systematics of a Paleoproterozoic cap-carbonate sequence from the Sausar Group, Central India. Palaeogeography, Palaeoclimatology, Palaeoecology 417, 95-209.

Mount, J.F. and Kidder, D., 1993. Combined flow origin of edgewise intraclast conglomerates, Sellick Hill Formation (Lower Cambrian), South Australia. Sedimentology 40, 315–329.

Myrow, P.M., Tice, L., Archuleta, B., Clark, B., Taylor, J.F. and Ripperdan, R.L., 2004. Flat pebble conglomerate: its multiple origins and relationship to meter-scale depositional cycles. Sedimentology 51, 973-996.

Nagarajan, R., Madhavaraju, J., Armstrong-Altrin, J.S. and Nagendra, R., 2011. Geochemistry of Neoproterozoic limestones of the Shahabad Formation, Bhima Basin, Karnataka, southern India. Geosciences Journal 15, 9-25.

Nesbitt, H.W. and Young, G.M., 1982. Early Proterozoic climates and plate motions inferred from major element chemistry of lutites. Nature 299, 715–717.

Nittrouer, C.A. and Wright, L.D., 1994. Transport of particles across continental shelves. Review of Geophysics 32, 85-113.

Nozaki, Y., Zhang, J. and Amakawa, H., 1997. The fractionation between Y and Ho in the marine environment. Earth and Planetary Science Letters 148, 329-340.

Nutz, A., Ghienne, J.-F., Schuster, M., Dieteich, P., Roquin, C., Hay, M.B., Bouchette, F. and Cousineau, P.A., 2015. Forced regressive deposits of a deglaciation sequence: Example from the Late Quaternary succession in the Lake Saint-Jean basin (Quebec, Canada). Sedimentology 62, 1573-1610.

Omar, G.I., Steckler, M.S, Buck, R. and Kohn, B.P., 1989. Fisson-track analysis of basement apatites at the western margin of the Gulf of Suez rift, Egypt: evidence for synchroneity of uplift and subsidence. Earth and Planetary Science Letters 94, 316-328.

Orton, G.J. and Reading, H.G., 1993, Variability of deltaic processes in terms of sediment supply, with particular emphasis on grain size: Sedimentology 40, 475– 512.

Ori, G.G., 1989. Geological history of the extensional basin of the Gulf of Corinth (Miocene-Pleistocene), Greece. Geology 17, 918-921.

Papineau, D., Mojzsis, S.J. and Schmitt, A.K., 2007. Multiple sulfur isotopes from Paleoproterozoic Huronian interglacial sediments and the rise of atmospheric oxygen. Earth and Planetary Science Letters 255, 188–212.

Parviainen, E.A.U., 1973. The sedimentology of the Huronian Ramsay Lake and Bruce Formations, north shore of Lake Huron, Ontario, Ph.D thesis, University of Western Ontario, London, Ontario, 426p.

Piepgras, D.J. and Jacobsen, S.B., 1992. The behavior of rare earth elements in seawater; precise determination of variations in the North Pacific water column. Geochimica et Cosmochimica Acta 56 (5), 1851-1862.

Pik, R., Marty, B., Carignan, J., Yirgu, G. and Ayalew, T., 2008. Timing of East African rift development in southern Ethiopia: Implications for mantle plume activity and evolution of topography. Geology 36, 167-170.

Planavsky, N., Bekker, A., Rouxel. O.J., Kamber, B., Hofmann, A., Knudsen, A. and Lyons, T., 2010. Rare Earth Element and yttrium compositions of Archean and Paleoproterozoic Fe formations revisited: New perspectives on the significance and mechanism of deposition. Geochimica et Cosmochimica Acta 74, 6387-6405.

Plint, A.G., 2010. Wave- and storm-dominated shoreline and shallow-marine systems. In: James, N.P., Dalrymple, R.W. (Eds.), Facies Models 4. Geological Association of Canada, Newfoundland, Canada, 167-199.

Polteau, S., Moore, J.M and Tsikos, H., 2006. The geology and geochemistry of the Paleoproterozic Makganyene diamictite. Precambrian Research 148, 257-274.

Quirke, T.T., 1917. Espanola District, Ontario. Canadian Geological Survey Memoir 102, 92p.

Rasmussen, B., Buick, R. andTayler, W.R., 1998. Removal of oceanic rare earth elements by authigenic precipitation of phosphatic minerals. Earth and Planetary Science Letters 164,135-149.

Rasmussen, B., Bekker, A. and Fletcher, I.R., 2013. Correlation of Paleoproterozoic glaciations based on U-Pb zircon ages for tuff beds in the Transvaal and Huronian Supergroups. Earth and

Planetary Science Letters 382, 173-180.

Rieu, R., Allen, P.A., Etienne, J.L., Cozzi, A. and Wiechert, U., 2006. A Neoproterozoic glacially influenced basin margin succession and “atypical” cap carbonate associated with bedrock palaeovalleys, Mirbat area, southern Oman. Basin Research 18, 471–496.

Roberts, S., Palmer, M.R., Cooper, M.J., Bucaus, P. and Sargent, D., 2009. REE and Sr isotope characteristics of carbonate within the Cu-Co mineralized sedimentary sequence of the Nchanga Mine, Zambian Copperbelt. Mineria Deposita 44, 881-891.

Robertson, J.A., 1964. Geology of Scarfe, Mack, Cobden and Striker Townships, District of Algoma. Ontario Department of Mines Geological Report 20, 89p.

Robertson, J.A., 1968. Geology of Township 149 and Township 150. Ontario Department of Mines Geological Report 57, 1-162.

Rodler, A.S., Frei, R., Gaucher, C. and Germs, G.J.B., 2016. Chromium isotopes, REE and redox-sensitive element chemostratigraphy across the late Neoproterozoic Ghaub glaciation, Otavi Group, Namibia. Precambrian Research 186, 234-249.

Roscoe, S.M., 1969. Huronian rocks and uraniferous conglomerates in the Canadian Shield. Geologic Survey of Canada Paper 68-40, 205p.

Roscoe, S.M., 1973. The Huronian Supergroup, a Paleoaphebian succession showing evidence of atmospheric evolution. In, Huronian Stratigraphy and Sedimentation. Geological Association of Canada special volume 12, 31-38.

Rothman, D.H., Hayes, J.M. and Summons, R.E., 2003. Dynamics of the Neoproterozoic carbon cycle. PNAS, USA 100, 8124–8129.

Royden, L. and Keen, C.E., 1980. Rifting process and thermal evolution of the continental margin of eastern Canada determined from subsidence curves. Earth and Planetary Science Letters 51, 343-361.

Royden L., Sclater, J.G. and Von Herzen, R.P., 1980. Continental margin subsidence and heat flow; important peramiters in formation of petroleum hydrocarbons. Americal Association of Petroleum Geologists 64, 173-187.

Sarangi, S., Mohanty, S.P. and Barik, A., 2017. Rare earth element characteristics of Paleoproterozoic cap carbonates pertaining to the Sausar Group, Central India: implications for ocean paleoredox conditions. Journal of Asian Earth Sciences 148, 31-50.

Sawlowicz, Z., 2013. REE and their relevance to the development of the Kupferschiefer copper deposit in Poland. Ore Geology Reviews 55, 176-186.

Sekine, Y., Suzuki, K., Senda, R., Goto, K.T., Tajika, E., Tada, R., Goto, K., Yamamoto, S.,

Ohkouchi, N., Ogawa, N.O. and Maruoka, T., 2011. Osmium evidence for synchronicity between a rise in atmospheric oxygen and Palaeoproterozoic deglaciation. Nature Communications 2, 502.

Selley, D., Broughton, D., Scott, R., Hitzman, M., Bull, S.W., Large, R.R., McGoldrick, P.J., Croaker, M., Pollington, N. and Barra, F., 2005. A new look at the geology of the Zambian Copperbelt. Economic Geology, 100, p. 965-1000.

Sellwood, B.W. and Netherwood, R.E., 1984. Facies evolution of the Gulf of Suez area; sedimentation history as an indicator of rift initiation and development. Modern Geology 1, 43-69.

Shen, Y., Zhang, T. and Chu, X., 2005. C-isotopic stratification in a Neoproterozoic postglacial ocean. Precambrian Research 137, 243–251.

Sepkoski, J.J., 1982. Flat-pebble conglomerates, storm deposits, and the Cambrian bottom fauna. In: Cyclic Event and Stratification (Eds G. Einsele and A. Seilacher), Springer-Verlag, Berlin, 371–388.

Shields, G.A., 2005. Neoproterozoic cap carbonates: a critical appraisal of existing models and the plumeworld hypothesis. Terra Nova 17, 299-310.

Shields, G.A., Deynoux, M., Strauss, H., Paquet, H., and Nahon, D., 2007. Barite-bearing cap dolostones of the Taoudéni Basin, northwest Africa: Sedimentary and isotopic evidence for methane seepage after a Neoproterozoic glaciation. Precambrian Research 153, 209–235.

Sholkovitz, E. R., Landing, W. M. and Lewis, B. L., 1994. Ocean particle chemistry – the fractionation of rare-earth elements between suspended particles and seawater. Geochimica et Cosmochimica Acta 58, 1567–1579.

Simonson, B.M., Schubel, K.A. and Hassler, S.W., 1993. Carbonate sedimentology of the early Precambrian Hamersley Group of Western Australia. Precambrian Research 60, 287–335.

Sleep, N.H., 1971. Thermal effects of the formation of Atlantic continental margins by continental breakup. Geophysical Journal of the Royal Astronomical Society 24, 325-350.

Smith, D.J. and Hopkins, T.S., 1972. Sediment transport on the continental shelf of Washington and Oregon in light of recent current measurements. In, Ed. by D.P.J. Swift, D.B Duane and O.H. Pilkey, Shelf Sediment Transport: Process and Pattern, Dowden, Hutchison and Ross, Stroudsbourg, 143-180.

Soyol-Erdene, T.-O. and Huh, Y., 2013. Rare earth element cycling in the pore waters of the Bearing Sea slope. Chemical Geology 358, 75-89.

Steckler, M.S., 1985. Uplift and extension at the Gulf of Suez: indications of induced mantel convection. Nature 317, 135-139.

Steckler, M.S. and Omar, G.I., 1994. Controls on erosional retreat of the uplifted rift flanks at the Gulf of Suez and northern Red Sea. Journal of Geophysipal Research 99, 12159-12173.

Steckler, M.S. and Watts, A.B., 1978. Subsidence of the Atlantic-type continental margin off New York. Earth and Planetary Science Letters 41, 1-13.

Strand, K.O. and Laajoki, K., 1993. Paleoproterozoic Paleomarine sedimentation in an extensional tectonic setting: the Honkala Formation, Finland. Precambrian Research 64, 253-271.

Sumner, D.Y. and Grotzinger, J.P., 2000. Late Archean aragonite precipitation: petrography, facies associations, and environmental significance. In: Grotzinger, J.P., James, N.P. (Eds.), Carbonate Sedimentation and Diagenesis in the Evolving Precambrian World, 67. SEPM Special Publication, 123–144.

Surya Prakash, L., Ray, D., Paropkari, A.L., Mudholkar, A.V., Satyanarayanan, M., Sreenivas, B., Chandrasekharam, D., Kota, D., Kamesh Raju, K.A., Kaisary, S., Balaram. V. and Gurav, T., 2012. Distribution of REEs and yttrium among geochemical phases of marine Fe-Mn oxides: Comparative study between hydrogenous and hydrothermal deposits. Chemical Geology 312-313, 127-137.

Taylor, S.R. and McLennan, S.M., 1985. The Continental Crust: its Composition and Evolution; an Examination of the Geochemical Record Preserved in Sedimentary Rocks. Blackwell, Oxford.

Thiessen, R., Burke and K. and Kidd, W.S.F., 1979. African hotspots and their relation to the underlying mantle. Geology 7, 263-266.

Van Kranendonk, M.J., Webb, G.E. and Kamber, B.S., 2003. Geological and trace element evidence for a marine sedimenarty environmentof deposition and biogenicity of 3.45 Ga stromatolitic carbonates in the Pilbara craton, and support for a reducing Archean ocean. Geobiology 1, 91-108.

Van Schmus, W.R., 1965. The geochronology of the Blind River-Bruce Mines area, Ontario. Journal of Geology 73, 755-780.

Van Schmus, W.R., 1976. Early and Middle Proterozoic history of the Great Lakes area, North America. In: Glogal Tectonics in Proterozoic Time. Philosophical Transactions of the Royal Society ofLondon, Series A, 280, 605-628.

Veizer, J., Clayton, R.N. and Hinton, R.W., 1992. Geochemistry of Precambrian carbonates; IV, Early Paleoproterozoic (2.25 + or - 0.25 Ga) seawater. Geochimica et Cosmochimica Acta 56, 875-885.

Vennemann, T.W., Kesler, S.E., Frederickson, G.C., Minter, W.E.L. and Heine, R.R., 1996. Oxygen isotope sedimentology of gold- and uranium-bearing Witwatersrand and Huronian Supergroup quartz-pebble conglomerates. Economic Geology, 91, 322-342.

Verdel, C., Phelps, B. and Walsh, K., 2018. Rare earth element and $^{87}Sr/^{86}Sr$ step leaching geochemistry of central Australian Neoproterozoic carbonates. Precambrian Research 310, 229-242.

Viehmann, S., Bau, M., Hoffmann, J.E. and Munker, C., 2015. Geochemistry of the Krivoy Roy banded iron formation, Ukraine, and the impact of peaked episodes of increased global magmatic activity on the trace element composition of Precambrian seawater. Precambrian Research 270, 165-180.

Wade, J.A. and MacLean, B.C., 1990. Chapter 5 – The geology of the southeastern margin of Canada, part 2: aspects of the geology of the Scotia Basin from recent seismic and well data. In, ed. By M.J. Keen and G.L. Williams, Geology of Canada No. 2 – Geology of the Continental Margin of Eastern Canada, vol. 2. Geological Survey of Canada, 190-238.

Wade, J.A., MacLean, B.C. and Williams, G.L., 1995. Mesozoic and Cenozoic stratigraphy, eastern Scotian Shelf: new interpretations. Canadian Journal of Earth Sciences 32, 1462-1473.

Wang, J., Jiang, G., Xiao, S., Li, Q. and Wei, Q., 2008. Carbon isotope evidence for widespread methane seeps in the ca. 635 Ma Doushantuo cap carbonate in south China. Geology 36, 347–350.

Warke, M.R., Rocco, T.D., Zerkle, A.L., Lepland, A., Prave, A.R., Martin, A.P., Ueno, Y., Condon, D.J. and Claire, M.W., 2020. The Great Oxidation Event preceded a Paleoproterozoic "snowball Earth". PNAS 117, 13314-13320.

Wei, G., Van Smeerdijk Hood, A., Chen, X., Li, D., Wei, W., Wen, B., Gong, Z., Yang, T., Zhang, Z. and Ling, H., 2019. Ca and Sr isotope constraints on the formation of the Marinoan cap dolostones. Earth and Planetary Science Letters 511, 202-212.

Wen B., Evans, D.a.d., Li, Y., Wang, Z. and Liu, C., 2015. Newly discovered Neoproterozoic diamictite and cap carbonate (DOC) couplet in Tarim Craton, NW China; stratigraphy, geochemistry, and paleoenvironment. Precambrian Research 271, 278-294.

Williams, G.E. and Schmidt, P.W., 1997. Paleomagnetism of the Paleoproterozoic Gowganda and Lorrain Formations, Ontario: Low paleolatitude for Huronian glaciation. Earth and Planetary Science Letters 153, 157-169.

Williams, G.E., and Schmidt, P.W., 2018. Shuram–Wonoka carbon isotope excursion: Ediacaran revolution in the world ocean's meridional overturning circulation. Geoscience Frontiers 9, 391–402.

Wilson, M.D., 1985. Origin of Upper Cambrian flat pebble conglomerates in the Northern Powder River Basin, Wyoming. 7th SEPMCore Workshop. Golden, CO, 1–50.

Wilson, R.C.L., 1975. Atlantic opening and Mesozoic continental margin basins of Iberia. Earth and Planetary Science Letters 94, 316-328.

Yoshioka, H., Asahara, Y., Tojo, B. and Kawakami, S., 2003. Systematic variations in C, O, and Sr isotopes and elemental concentrations in Neoproterozoic carbonates in Namibia; implications for a glacial to interglacial transition. Precambrian Research 124, 69-85.

Young, G.M., 1973. Origin of carbonate-rich Early Proterozoic Espanola Formation, Ontario, Canada. Geological Society of America Bulletin 84, 135–160.

Young, G.M., 2004. Earth's earliest extensive glaciations: tectonic setting and stratigraphic context of Paleoproterozoic glaciogenic deposits. In: Jenkins, G.S., McMenamin, M.A.S., McKay, C.P., Sohl, L. (Eds.), The Extreme Proterozoic: Geology, Geochemistry and Climate. American Geophysical Union, Washington, DC, Geophysical Monograph 146,

161-181.

Young, G.M., 2013a. Precambrian supercontinents, glaciations, atmospheric oxygenation, metazoan evolution and an impact that may have changed the second half of Earth history. Geoscience Frontiers 4, 247-261.

Young, G.M., 2013b. Climatic catastrophes in Earth history: two great Proterozoic glacial episodes. Geological Journal 48, 1-21.

Young, G.M., 2014. Contradictory correlations of Paleoproterozoic glacial deposits: Local, regional or global controls? Precambrian Research 247, 33-44.

Young, G.M. and Nesbitt, H.W., 1985. The Gowganda Formation in the southern part of the Huronian outcrop belt, Ontario, Canada; stratigraphy, depositional environments and regional tectonic significance. Precambrian Research 29, 265-301.

Young, G. M., Long D.G.F., Fedo C.M. and Nesbitt H.W., 2001. Paleoproterozoic Huronian basin: product of a Wilson cycle punctuated by glaciations and a meteorite impact. Sedimentary Geology 141-142, 233-254.

Yu, Z., Colin, C., Meynadier, L., Douville, E., Dapoigny, A., Reverdin, G., Wu, Q., Wan, S., Song, L., Xu, Z. and Bassinot, F, 2017. Seasonal variations in dissolved Neodymium isotope composition in the Bay of Bengal. Earth and Planetary Science Letters 479, 310-321.

Zahnle, K., Claire, M. and Catling, D., 2006. The loss of mass-independent fractionation in sulfur due to a Paleoproterozoic collapse of atmospheric methane. Geobiology 4, 271-283.

Zhang, J. and Nozaki, Y., 1996. Rare earth elements and yttrium in seawater; ICP-MS determinations in the East Caroline, Coral Sea, and South Fuji basins of the western South Pacific Ocean. Geochimica et Cosmochimica Acta 60, 4631-4644.

Zhang, S., Jiang, G. and Han, Y., 2008. The age of the Nantuo Formation and Nantuo glaciation in South China. Terra Nova 20, 289-294.

Zhao, Y.-Y. and Zheng, Y.-F., 2013. Geochemical constraints on the origin of post-depositional fluids in sedimentary carbonates of the Ediacaran system in South China. Precambrian Research 224, 341-363.

Zao, Y.Y., Zheng, Y.F. and Chen, F., 2009. Trace element and strontium isotope constraints on sedimentary environment of Ediacaran carbonates in southern Anhui, China. Chemical Geology 265, 345-362.

Figures

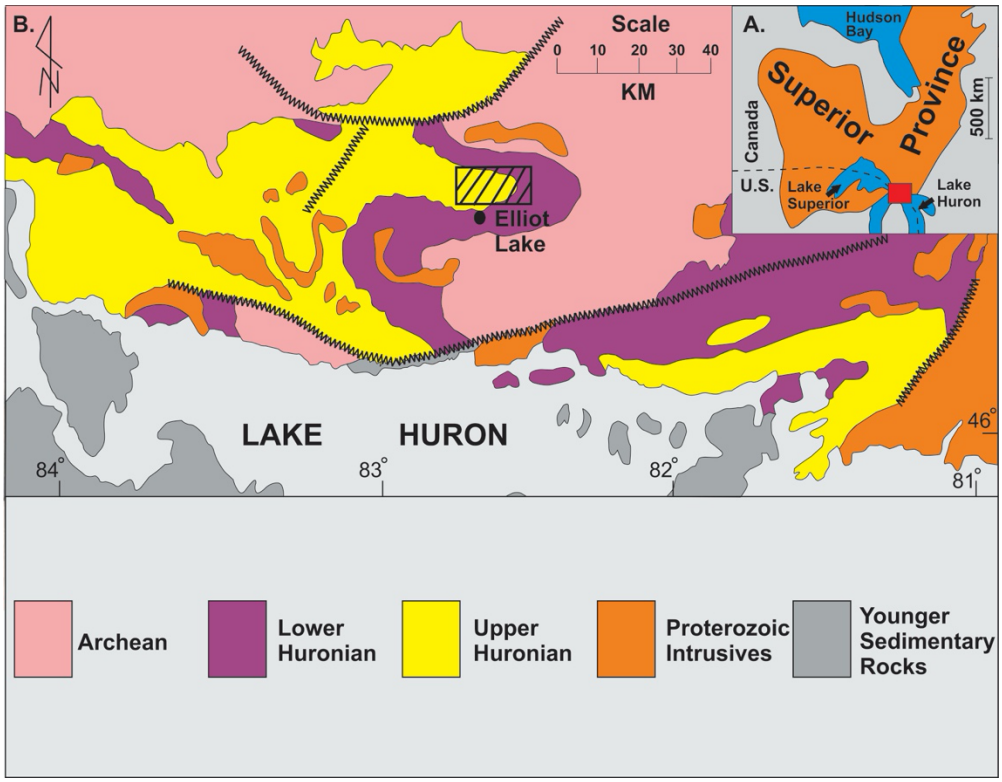

Figure 1. A. Location map of the Huronian Supergroup, red rectangle, in Canada north of the Great Lakes in the central area of the continent. B. The rectangle near Elliot Lake is the location of four cored drill-holes that are discussed in the text. The Lower Huronian includes Formations up to the base of the Gowganda Formation. The Upper Huronian includes the Gowganda and overlying Formations.

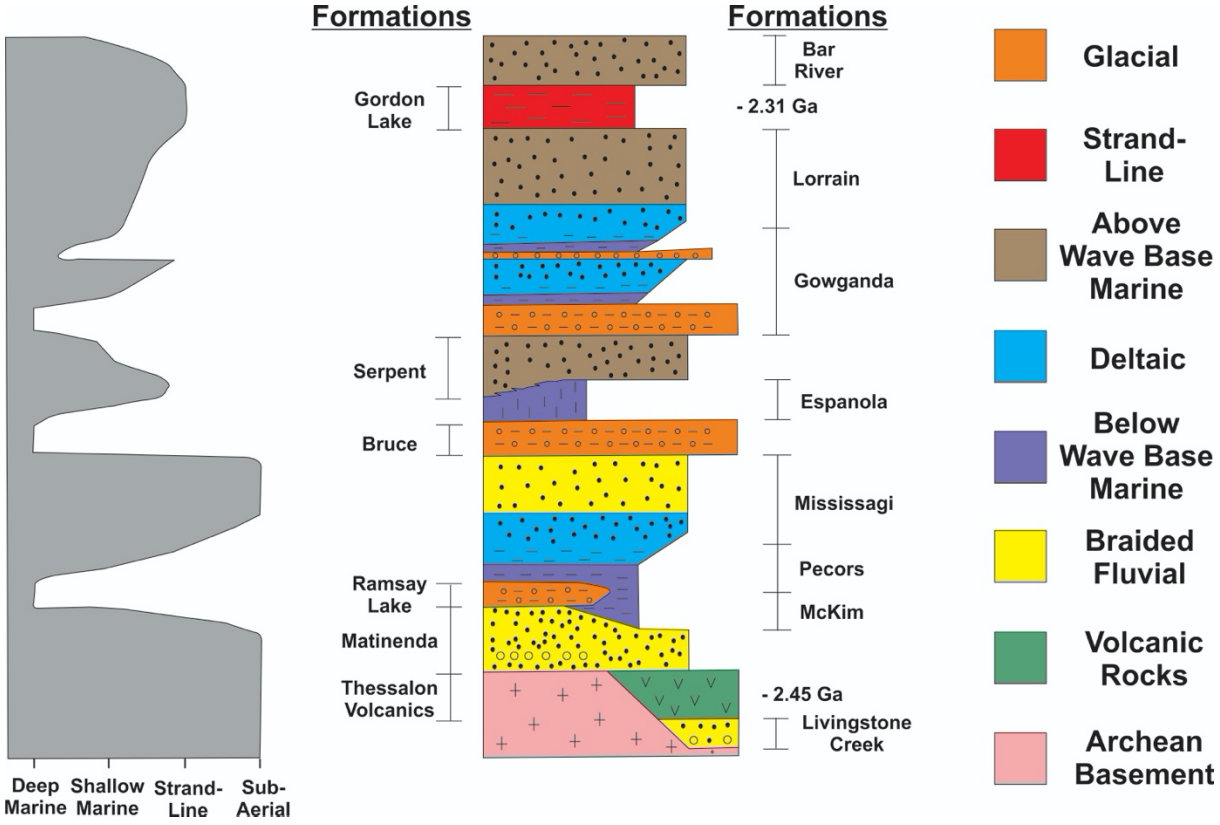

Figure 2. Stratigraphic section of the Huronian Supergroup. The thickness of most Formations increases from north to south over a present day horizontal distance of 60 kilometers, culminating in over 10 kilometers of section. Basinal changes in relative sea-level, depicted on the left side of the diagram, are discussed in the Regional Geology section of the text. The flooding events are related to isostatic loading by advancing ice sheets.

Figure 3. A) Typical Bruce Formation diamictite. B) Glacial dropstone penetrating and compressing siltstone (S) and limestone (C) layers. Ice dropped debris is present in the siltstone-carbonate unit between glacial diamictite layers in Figure 4. Coin is 1.9 cm. C) Sharp contact

between Bruce diamictite (G), 20cm of siltstone (L) and overlying Espanola carbonate (C) with thin siltstone layers. D) Outcrop of parallel laminated limestone and siltstone. Hammer is 30cm. E) Wave ripple laminated iron-rich dolostone with dark, fine-grained siliciclastics. F) Iron-rich dolostone (D) and interlayered sandstone (S) near the top of the Espanola Formation.

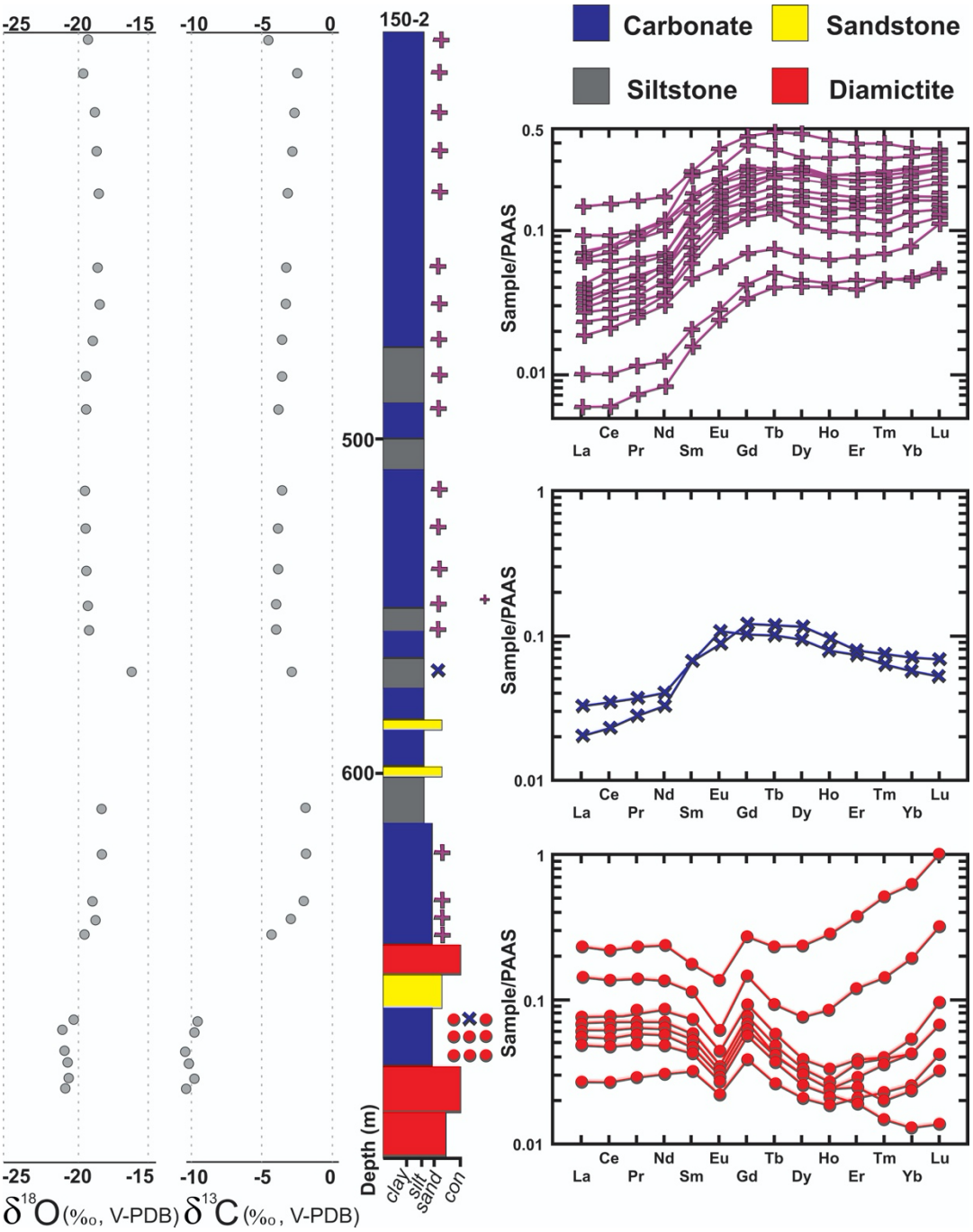

Figure 4. Stratigraphic section for drill hole E150-2. $\delta^{13}C_{carb}$ and $\delta^{18}O$ isotopic data are plotted in accordance with their position on the stratigraphic column to visualize trends. Carbonate layers during glacial deposition (red dots) have very light carbon. As glacial processes waned carbon isotopes became heavier, increasing from -10‰ to -2‰. At 60 meters above the last ice rafted debris the isotopic ratio decreases from -2‰ to -4‰ and then incrementally increases to -2.5‰ over the next 150 meters. The abundance patterns for REEs have three distinct shapes, which in part correlate with the C isotopic data. Injection breccia and slumped units are not portrayed in the section. The carbonate is interlayered with siliciclastics, whereas the siltstones have a smaller carbonate component.

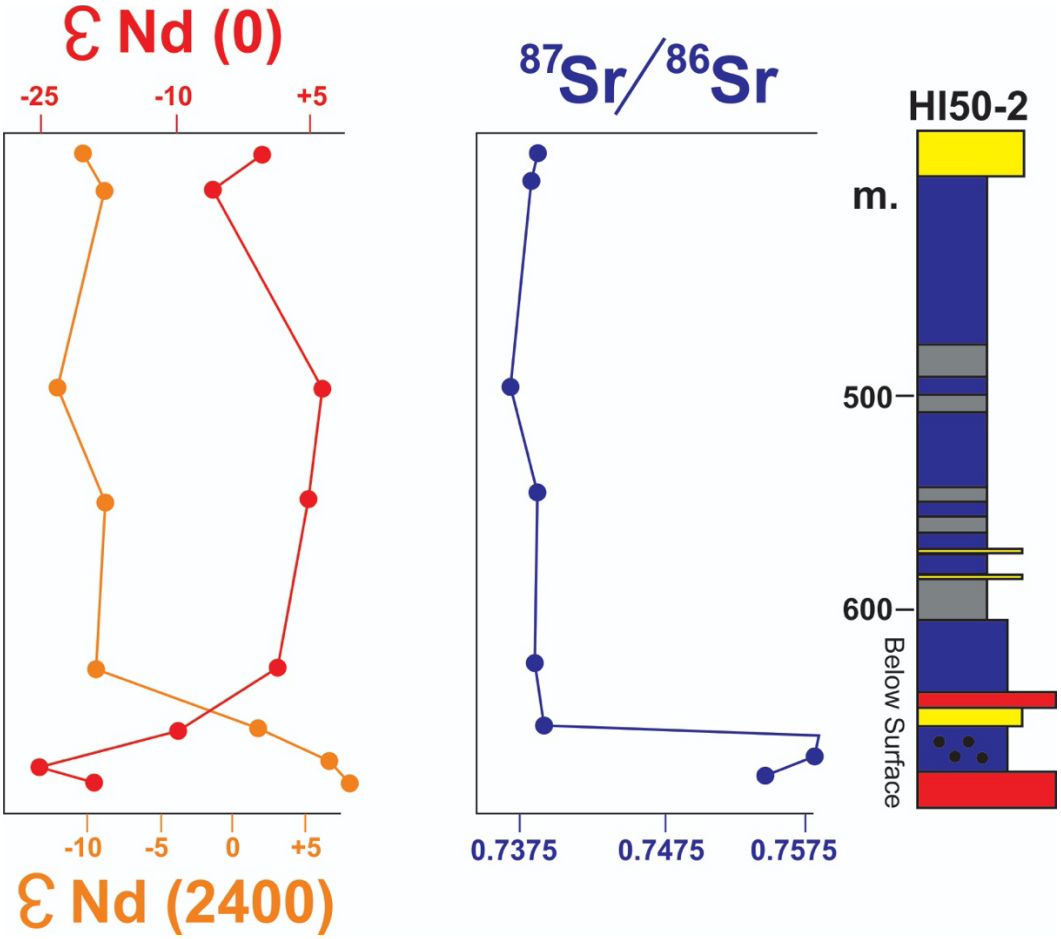

Figure 5. $^{87}Sr/^{86}Sr$, ε(0) Nd and ε(2400)Nd values plotted with their sample position from drill-hole 150-2. The lowest blue unit represents the carbonate with glacial rainout debris. The trends are discussed in the text.

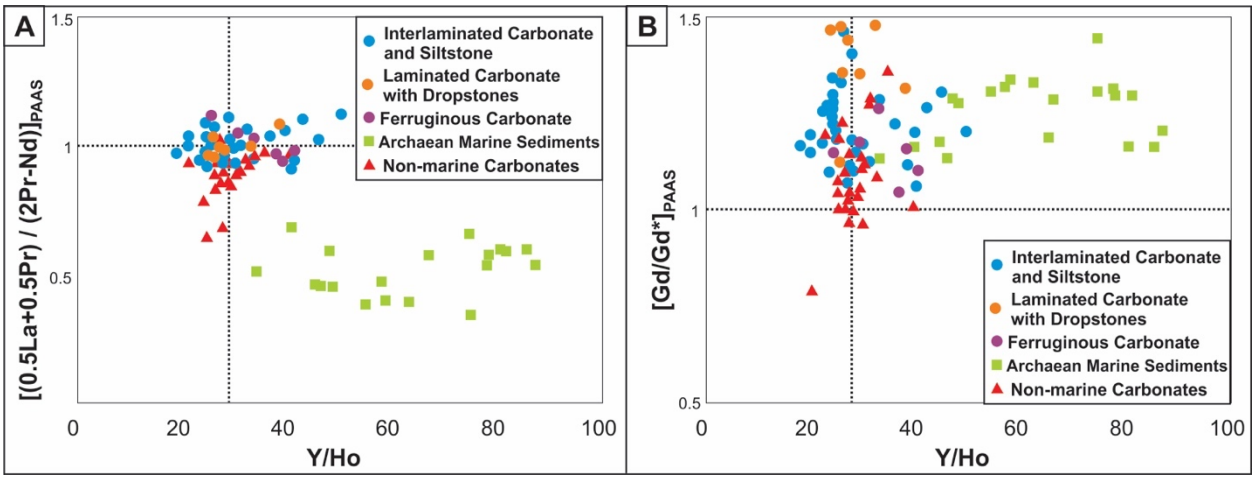

Figure 6. Y/Ho ratios of Espanola samples compared to fields for Precambrian non-marine and marine samples. Espanola samples mainly fall in the freshwater field. Diagram type developed by Hu et al. (2016), with original non-marine and marine data from Van Kranendonk et al. (2003), Bolhar et al. (2004), Bolhar and Van Kranendonk (2007), Zhao et al. (2009) and Huang et al. (2011).

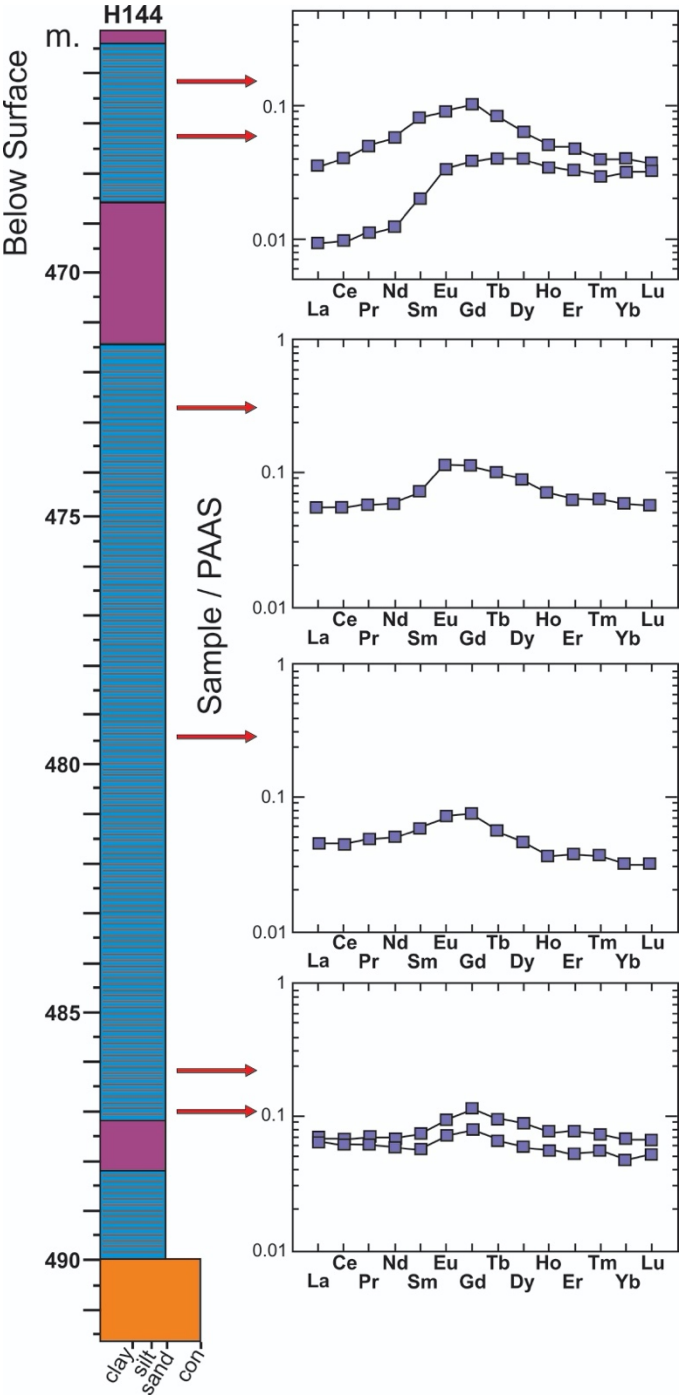

Figure 7. REE patterns of carbonate samples from the interlaminated carbonate and siltstone lithofacies association in drill hole 144-1. The lowest sample is 3m above the Bruce diamictite. The relatively flat patterns at the base of section become more MREE enriched and LREE depleted with stratigraphic height. The patterns for the highest samples in this diagram are

typical of the two present lower in the laminated carbonate – siltstone succession in Figure 4. REE patterns for samples from stratigraphically above these (Figure 4) have more pronounced LREE depletion and very slight to no MREE enrichment.

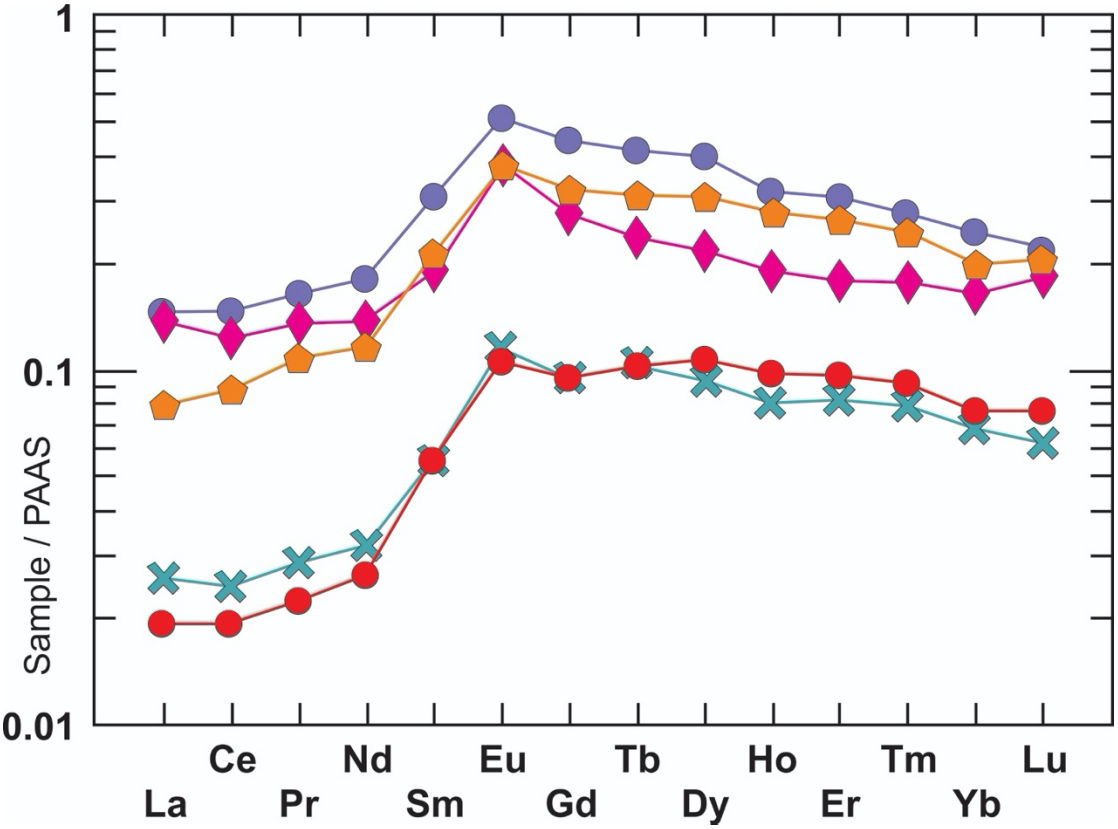

Figure 8. PAAS normalized REE patterns of iron-rich dolomites in the northern outcrop area. This lithology is associated with probable shallow water microbialites in the upper Espanola Formation. It is also the only lithofacies with positive Eu anomalies. They range from 1.5 to 1.8 (Eu/((0.67Sm*)+(0.33Tb*)), *=PAAS normalized, Bau and Dulski 1996), typical for sea water at this time (Viehmann et al., 2015, Fig. 10).

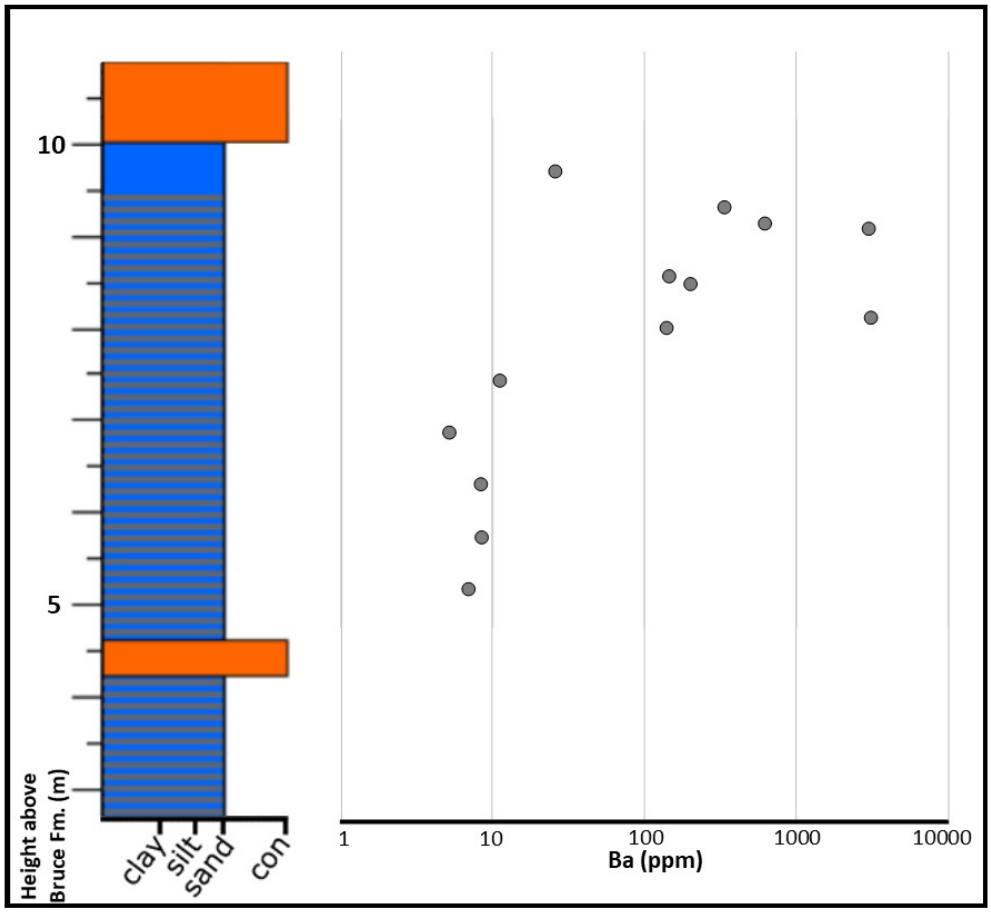

Figure 9. Between 8 and 9.5 meters above the main diamictite unit in drill-hole E150-1 Ba concentrations increase from approximately 9 to over 1000 ppm in the carbonate fraction of samples. Similar zones of extreme Ba values are present in Neoproterozoic cap carbonates.